



Vande Sadguram Chandrasekharam



श्रीचन्द्रशेखरेन्द्रसरस्वतीविश्वमहाविद्यालयः
SRI CHANDRASEKHARENDRASARASWATHI VISWA MAHAVIDYALAYA

Deemed to be University of UGC Act 1956 | Accredited with "A" grade by NAAC
Enathur, Kanchipuram - 631 561, Tamilnadu, India | www.kanchiuniv.ac.in
Sponsored and run by Sri Kanchi Kamakoti Peetam Charitable Trust



STUDY MATERIAL
of
MOBILE COMMUNICATION AND NETWORKS

DEPARTMENT OF ELECTRONICS AND COMMUNICATION ENGINEERING

Prepared by: Dr.S.Selvakumar
Assistant Professor



Sri Chandrasekharendra Saraswathi Viswa Mahavidyalaya
Department of Electronics and Communication Engineering
Syllabus for Full Time BE, Regulations 2018
(Applicable for students admitted from 2018-19 onwards)

PEC4 MOBILE COMMUNICATION AND NETWORKS VII SEMESTER

PRE-REQUISITE:

Basic knowledge of Digital Communication and Antennas

L	T	P	C
3	0	0	3

OBJECTIVES:

- To understand the issues involved in mobile communication system design and analysis.
- To understand the concept of frequency reuse.
- To understand the characteristics of wireless channels.
- To know the fundamental limits on the capacity of wireless channels.

UNIT I CELLULAR CONCEPTS

(8 Hrs)

Cellular concepts- Cell structure, frequency reuse, cell splitting, channel assignment, handoff, interference, capacity, power control; Wireless Standards: Overview of 2G and 3G cellular standards.

UNIT II THE WIRELESS CHANNEL

(10 Hrs)

Signal Propagation-Propagation mechanism- reflection, refraction, diffraction and scattering, large scale signal propagation and lognormal shadowing. Fading channels -Multipath and small scale fading- Doppler shift, statistical multipath channel models, narrowband and wideband fading models, power delay profile, average and rms delay spread, coherence bandwidth and coherence time, flat and frequency selective fading, slow and fast fading, average fade duration and level crossing rate.

UNIT III ANTENNAS FOR MOBILE TERMINALS

(9 Hrs)

Capacity of flat and frequency selective channels, Antennas- Antennas for mobile terminal monopole antennas, PIFA, base station antennas and arrays

UNIT IV MULTI-ANTENNA COMMUNICATION

(9 Hrs)

Receiver structure- Diversity receivers- selection and MRC receivers, RAKE receiver, equalization: linear-ZFE and adaptive, DFE. Transmit Diversity-Altamonte scheme.

UNIT V MIMO AND MULTIPLEXING

(9 Hrs)

MIMO and space time signal processing, spatial multiplexing, diversity/multiplexing tradeoff. Performance measures- Outage, average SNR, average symbol/bit error rate. System examples- GSM, EDGE, GPRS, IS-95, CDMA 2000 and WCDMA

OUTCOMES:

Total: 45 Hrs

At the end of the course, students will demonstrate the ability to -

- Understand the working principles of the mobile communication systems.
- Understand the relation between the user features and underlying technology.
- Analyze mobile communication systems for improved performance.

TEXT/REFERENCE BOOKS:

1. WCY Lee, Mobile Cellular Telecommunications Systems, McGraw Hill, 1990.
2. WCY Lee, Mobile Communications Design Fundamentals, Prentice Hall, 1993.
3. Raymond Steele, Mobile Radio Communications, IEEE Press, New York, 1992.
4. AJ Viterbi, CDMA: Principles of Spread Spectrum Communications, Addison Wesley, 1995.
5. VK Garg&JE Wilkes, Wireless & Personal Communication Systems, Prentice Hall, 1996

Unit-I : The Cellular Concept-

System Design Fundamentals

Introduction

We have seen that the technique of substituting a single high power transmitter by several low power transmitters to support many users is the backbone of the cellular concept. In practice, the following four parameters are most important while considering the cellular issues: system capacity, quality of service, spectrum efficiency and power management. Starting from the basic notion of a cell, we would deal with these parameters in the context of cellular engineering in this chapter.

What is a Cell?

The power of the radio signals transmitted by the BS decay as the signals travel away from it. A minimum amount of signal strength (let us say, x dB) is needed in order to be detected by the MS or mobile sets which may be the hand-held personal units or those installed in the vehicles. The region over which the signal strength lies above this threshold value x dB is known as the coverage area of a BS and it must be a circular region, considering the BS to be isotropic radiator. Such a circle, which gives this actual radio coverage, is called the foot print of a cell (in reality, it is amorphous). It might so happen that either there may be an overlap between any two such side by side circles or there might be a gap between the

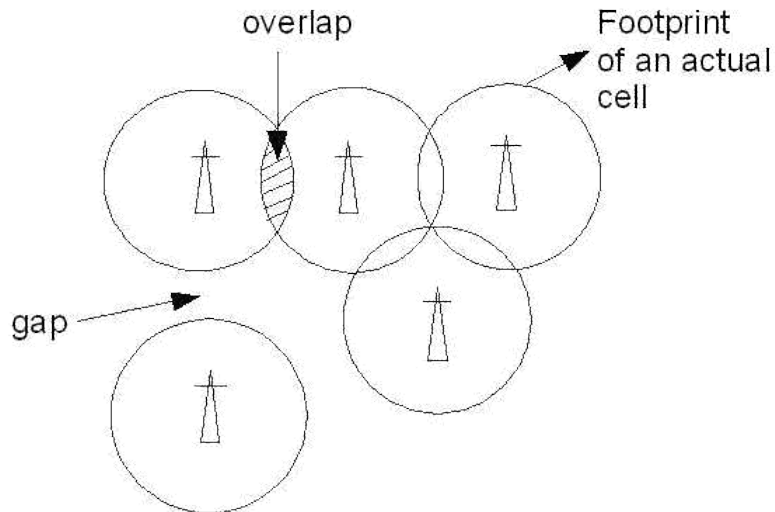


Figure 3.1: Footprint of cells showing the overlaps and gaps.

coverage areas of two adjacent circles. This is shown in Figure 3.1. Such a circular geometry, therefore, cannot serve as a regular shape to describe cells. We need a regular shape for cellular design over a territory which can be served by 3 regular polygons, namely, equilateral triangle, square and regular hexagon, which can cover the entire area without any overlap and gaps. Along with its regularity, a cell must be designed such that it is most reliable too, i.e., it supports even the weakest mobile with occurs at the edges of the cell. For any distance between the center and the farthest point in the cell from it, a regular hexagon covers the maximum area. Hence regular hexagonal geometry is used as the cells in mobile communication.

Frequency Reuse

Frequency reuse, or, frequency planning, is a technique of reusing frequencies and channels within a communication system to improve capacity and spectral efficiency. Frequency reuse is one of the fundamental concepts on which commercial wireless systems are based that involve the partitioning of an RF radiating area into cells. The increased capacity in a commercial wireless network, compared with a network with a single transmitter, comes from the

fact that the same radio frequency can be reused in a different area for a completely different transmission.

Frequency reuse in mobile cellular systems means that frequencies allocated to

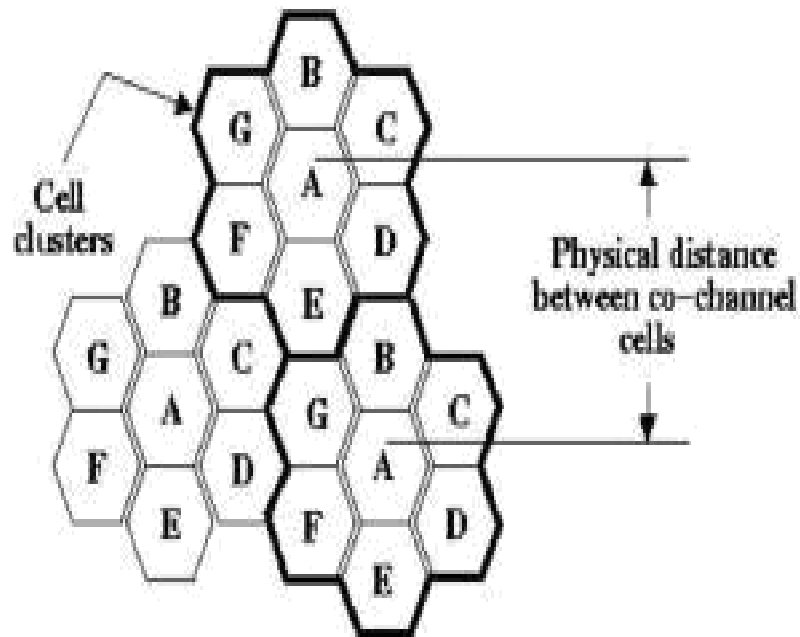


Figure 3.2: Frequency reuse technique of a cellular system

the service reused in a regular pattern of cells, each covered by one base station. The repeating regular pattern of cells is called cluster. Since each cell is designed to use radio frequencies only within its boundaries, the same frequencies can be reused in other cells not far away without interference, in another cluster. Such cells are called 'co-channel' cells. The reuse of frequencies enables a cellular system to handle a huge number of calls with a limited number of channels. Figure 3.2 shows a frequency planning with cluster size of 7, showing the co-channels cells in different clusters by the same letter. The closest distance between the co-channel cells (in different clusters) is determined by the choice of the cluster size and the layout of the cell cluster. Consider a cellular system with S duplex channels available for use and let N be the number of cells in a

cluster. If each cell is allotted K duplex channels with all being allotted unique and disjoint channel groups we have $S = KN$ under normal circumstances. Now, if the cluster are repeated M times within the total area, the total number of duplex channels, or, the total number of users in the

system would be $T = MS = KMN$. Clearly, if K and N remain constant, then

$$T \propto M \quad (3.1)$$

and, if T and K remain constant, then

$$N \propto \frac{1}{M} \quad (3.2) \quad \square$$

Hence the capacity gain achieved is directly proportional to the number of times a cluster is repeated, as shown in (3.1), as well as, for a fixed cell size, small N decreases the size of the cluster with in turn results in the increase of the number of clusters (3.2) and hence the capacity. However for small N, co-channel cells are located much closer and hence more interference. The value of N is determined by calculating the amount of interference that can be tolerated for a sufficient quality communication. Hence the smallest N having interference below the tolerated limit is used. However, the cluster size N cannot take on any value and is given only by the following equation

$$N = i^2 + ij + j^2, \quad i \geq 0, j \geq 0, \quad (3.3)$$

where i and j are integer numbers.

Channel Assignment Strategies

With the rapid increase in number of mobile users, the mobile service providers had to follow strategies which ensure the effective utilization of the limited radio spectrum. With increased capacity and low interference being the prime objectives, a frequency reuse scheme was helpful in achieving this objective . A variety of channel assignment strategies have been followed to aid these objectives. Channel assignment strategies are classified into two types: fixed and dynamic, as discussed below.

Fixed Channel Assignment (FCA)

In fixed channel assignment strategy each cell is allocated a fixed number of voice channels. Any communication within the cell can only be made with the designated unused channels of that particular cell. Suppose if all the channels are occupied, then the call is blocked and subscriber has to wait. This is simplest of the channel assignment strategies as it requires very simple circuitry but provides worst channel utilization. Later there was another approach in which the channels were borrowed from adjacent cell if all of its own designated channels were occupied. This was named as *borrowing strategy*. In such cases the MSC supervises the borrowing process and ensures that none of the calls in progress are interrupted.

Dynamic Channel Assignment (DCA)

In dynamic channel assignment strategy channels are temporarily assigned for use in cells for the duration of the call. Each time a call attempt is made from a cell the corresponding BS requests a channel from MSC. The MSC then allocates a channel to the requesting the BS. After the call is over the channel is returned

and kept in a central pool. To avoid co-channel interference any channel that in use in one cell can only be reassigned simultaneously to another cell in the system if the distance between the two cells is larger than minimum reuse distance. When compared to the FCA, DCA has reduced the likelihood of blocking and even increased the trunking capacity of the network as all of the channels are available to all cells, i.e., good quality of service. But this type of assignment strategy results in heavy load on switching center at heavy traffic condition.

Handoff Process

When a user moves from one cell to the other, to keep the communication between the user pair, the user channel has to be shifted from one BS to the other without interrupting the call, i.e., when a MS moves into another cell, while the conversation is still in progress, the MSC automatically transfers the call to a new FDD channel without disturbing the conversation. This process is called as *handoff*. A schematic diagram of handoff is given in Figure 3.3.

Processing of handoff is an important task in any cellular system. Handoffs must

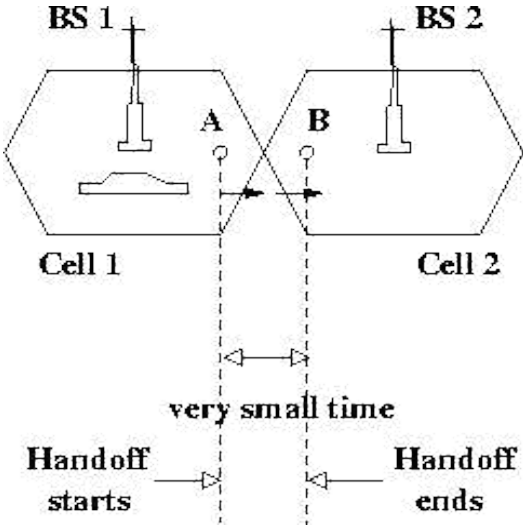


Figure 3.3: Handoff scenario at two adjacent cell boundary

Once a signal level is set as the minimum acceptable for good voice quality ($P_{r_{min}}$), then a slightly stronger level is chosen as the threshold (P_{r_H}) at which handoff has to be made, as shown in Figure 3.4. A parameter, called power margin, defined as

$$\Delta = P_{r_H} - P_{r_{min}} \quad (3.7)$$

is quite an important parameter during the handoff process since this margin Δ can neither be too large nor too small. If Δ is too small, then there may not be enough time to complete the handoff and the call might be lost even if the user crosses the cell boundary.

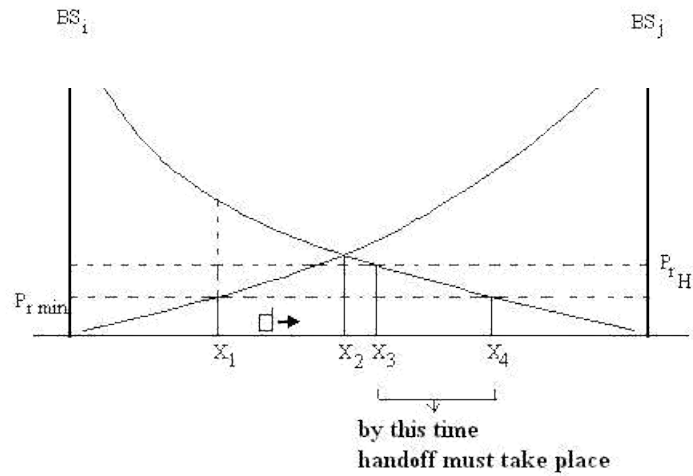
If Δ is too high on the other hand, then MSC has to be burdened with unnecessary handoffs. This is because MS may not intend to enter the other cell. Therefore Δ should be judiciously chosen to ensure imperceptible handoffs and to meet other objectives.

Factors Influencing Handoffs

The following factors influence the entire handoff process:

- (a) Transmitted power: as we know that the transmission power is different for different cells, the handoff threshold or the power margin varies from cell to cell.
- (b) Received power: depends on the Line of Sight (LoS) path between the user and the BS. Especially when the user the received power mostly is on the boundary of

hexagonal cell.



BS_i = Base station of i th cell
 BS_j = Base station of any adjacent j th cell

Figure 3.4: Handoff process associated with power levels, when the user is going from i -th cell to j -th cell.

the two cells, the LoS path plays a critical role in handoffs and therefore the power margin Δ depends on the minimum received power value from cell to cell.

(c) Area and shape of the cell: Apart from the power levels, the cell structure also plays an important role in the handoff process.

(d) Mobility of users: The number of mobile users entering or going out of a particular cell, also fixes the handoff strategy of a cell.

To illustrate the reasons (c) and (d), let us consider a rectangular cell with sides $R1$ and $R2$ inclined at an angle ϑ with horizon, as shown in the Figure 3.5. Assume $N1$ users are having handoff in horizontal direction and $N2$ in vertical direction per unit length.

The number of crossings along $R1$ side is : $(N1\cos\vartheta + N2\sin\vartheta)R1$ and the number of crossings along $R2$ side is : $(N1\sin\vartheta + N2\cos\vartheta)R2$.

Then the handoff rate λ_H can be written as

$$\lambda_H = (N_1 \cos\theta + N_2 \sin\theta)R_1 + (N_1 \sin\theta + N_2 \cos\theta)R_2. \quad (3.8)$$

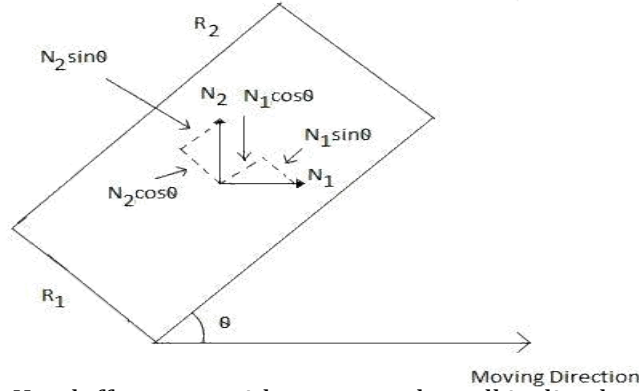


Figure 3.5: Handoff process with a rectangular cell inclined at an angle θ .

Now, given the fixed area $A = R_1 R_2$, we need to find λ_H^{opt} for a given θ . Replacing R_1 by $\frac{A}{R_2}$ and equating $\frac{d\lambda_H}{dR_1}$ to zero, we get

$$R_1^2 = A \left(\frac{N_1 \sin\theta + N_2 \cos\theta}{N_1 \cos\theta + N_2 \sin\theta} \right). \quad (3.9)$$

Similarly, for R_2 , we get

$$R_2^2 = A \left(\frac{N_1 \cos\theta + N_2 \sin\theta}{N_1 \sin\theta + N_2 \cos\theta} \right). \quad (3.10)$$

From the above equations, we have $\lambda_H = \frac{2}{\sqrt{A(N_1 N_2 + (N_1^2 + N_2^2) \cos\theta \sin\theta)}}$ which means it is minimized at $\theta = 0^\circ$. Hence $\lambda_H^{opt} = \frac{2}{\sqrt{A N_1 N_2}}$. Putting the value of θ in (3.9) or (3.10), we have $\frac{R_1}{R_2} = \frac{N_1}{N_2}$. This has two implications: (i) that handoff is

minimized if rectangular cell is aligned with X-Y axis, i.e., $\theta = 0^\circ$, and, (ii) that the number of users crossing the cell boundary is inversely proportional to the dimension of the other side of the cell. The above analysis has been carried out for a simple square cell and it changes in more complicated way when we consider a hexagonal cell.

Handoffs In Different Generations

In 1G analog cellular systems, the signal strength measurements were made by the BS and in turn supervised by the MSC. The handoffs in this generation can be termed as Network Controlled Hand-Off (NCHO). The BS monitors the signal strengths of voice channels to determine the relative positions of the subscriber. The special receivers located on the BS are controlled by the MSC to monitor the signal strengths of the users in the neighboring cells which appear to be in need of handoff. Based on the information received from the special receivers the MSC decides whether a handoff is required or not. The approximate time needed to make a handoff successful was about 5-10 s. This requires the value of Δ to be in the order of 6dB to 12dB.

In the 2G systems, the MSC was relieved from the entire operation. In this generation, which started using the digital technology, handoff decisions were mobile assisted and therefore it is called Mobile Assisted Hand-Off (MAHO). In MAHO, the mobile center measures the power changes received from nearby base stations and notifies the two BS. Accordingly the two BS communicate and channel transfer occurs. As compared to 1G, the circuit complexity was increased here whereas the delay in handoff was reduced to 1-5 s. The value of Δ was in the order of 0-5 dB. However, even this amount of delay could create a communication pause.

In the current 3G systems, the MS measures the power from adjacent BS and automatically upgrades the channels to its nearer BS. Hence this can be termed as Mobile Controlled Hand-Off (MCHO). When compared to the other generations, delay during handoff is only 100 ms and the value of Δ is around 20 dBm. The Quality Of Service (QoS) has improved a lot although the complexity of the circuitry has further increased which is inevitable.

All these types of handoffs are usually termed as hard handoff as there is a shift in the channels involved. There is also another kind of handoff, called soft handoff, as discussed below.

Handoff in CDMA: In spread spectrum cellular systems, the mobiles share the same channels in every cell. The MSC evaluates the signal strengths received from different BS for a single user and then shifts the user from one BS to the other without actually changing the channel. These types of handoffs are called as soft handoff as there is no change in the channel.

Handoff Priority

While assigning channels using either FCA or DCA strategy, a guard channel concept must be followed to facilitate the handoffs. This means, a fraction of total available channels must be kept for handoff requests. But this would reduce the carried traffic and only fewer channels can be assigned for the residual users of a cell. A good solution to avoid such a dead-lock is to use DCA with handoff priority (demand based allocation).

A Few Practical Problems in Handoff Scenario

(a) Different speed of mobile users: with the increase of mobile users in urban areas, microcells are introduced in the cells to increase the capacity (this will be discussed later in this chapter). The users with high speed frequently crossing the micro-cells become burdened to MSC as it has to take care of handoffs. Several schemes thus have been designed to handle the simultaneous traffic of high speed and low speed users while minimizing the handoff intervention from the MSC, one of them being the 'Umbrella Cell' approach. This technique provides large area coverage to high speed users while providing small area coverage to users traveling at low speed. By

using different antenna heights and different power levels, it is possible to provide larger and smaller cells at a same location. As illustrated in the Figure 3.6, umbrella cell is co-located with few other microcells. The BS can measure the speed of the user by its short term average signal strength over the RVC and decides which cell to handle that call. If the speed is less, then the corresponding microcell handles the call so that there is good corner coverage. This approach assures that handoffs are minimized for high speed users and provides additional microcell channels for pedestrian users.

(b) Cell dragging problem: this is another practical problem in the urban area with additional microcells. For example, consider there is a LOS path between the MS and BS1 while the user is in the cell covered by BS2. Since there is a LOS with the BS1, the signal strength received from BS1 would be greater than that received from BS2. However, since the user is in cell covered by BS2, handoff cannot take place and as a result, it experiences a lot of interferences. This problem can be solved by judiciously choosing the handoff threshold along with adjusting the coverage area.

(c) Inter-system handoff: if one user is leaving the coverage area of one MSC and is entering the area of another MSC, then the call might be lost if there is no handoff in this case too. Such a handoff is called inter-system handoff and in order to facilitate this, mobiles usually have roaming facility.

Interference & System Capacity

Susceptibility and interference problems associated with mobile communications equipment are because of the problem of time congestion within the electromagnetic spectrum. It is the limiting factor in the performance of cellular systems. This interference can occur from clash with another mobile in the same cell or because of a call in the adjacent cell. There can be interference between the base stations

operating at same frequency band or any other non-cellular system's energy leaking inadvertently into the frequency band of the cellular system. If there is an interference in the voice channels, cross talk is heard will appear as noise between the users. The interference in the control channels leads to missed and error calls because of digital signaling. Interference is more severe in urban areas because of the greater RF noise and greater density of mobiles and base stations. The interference can be divided into 2 parts: co-channel interference and adjacent channel interference.

Co-channel interference (CCI)

For the efficient use of available spectrum, it is necessary to reuse frequency bandwidth over relatively small geographical areas. However, increasing frequency reuse also increases interference, which decreases system capacity and service quality. The cells where the same set of frequencies is used are call co-channel cells. Co-channel interference is the cross talk between two different radio transmitters using the same radio frequency as is the case with the co-channel cells. The reasons of CCI can be because of either adverse weather conditions or poor frequency planning or overly-crowded radio spectrum.

If the cell size and the power transmitted at the base stations are same then CCI will become independent of the transmitted power and will depend on radius of the cell (R) and the distance between the interfering co-channel cells (D). If D/R ratio is increased, then the effective distance between the co-channel cells will increase and interference will decrease. The parameter Q is called the frequency reuse ratio and is related to the cluster size. For hexagonal geometry

$$Q = \frac{D}{R} = \sqrt{3N} \quad (3.11)$$

From the above equation, small of 'Q' means small value of cluster size 'N' and increase in cellular capacity. But large 'Q' leads to decrease in system capacity but increase in transmission quality. Choosing the options is very careful for the selection of 'N', the proof of which is given in the first section.

The Signal to Interference Ratio (SIR) for a mobile receiver which monitors the forward channel can be calculated as

$$\frac{S}{I} = \frac{S}{\sum_{i=1}^{i_0} I_i} \quad (3.12)$$

where i_0 is the number of co-channel interfering cells, S is the desired signal power from the baseband station and I_i is the interference power caused by the i-th interfering co-channel base station. In order to solve this equation from power calculations, we need to look into the signal power characteristics. The average power in the mobile radio channel decays as a power law of the distance of separation between transmitter and receiver. The expression for the received power P_r at a distance d can be approximately calculated as

$$P_r = P_0 \left(\frac{d}{d_0} \right)^{-n} \quad (3.13)$$

and in the dB expression as

$$P_r (\text{dBm}) = P_0 (\text{dBm}) - 10n \log \left(\frac{d}{d_0} \right) \quad (3.14)$$

P_0 is the power received at a close-in reference point in the far field region at a small distance d_0 from the transmitting antenna, and 'n' is the path loss exponent. Let us calculate the SIR for this system. If D_i is the distance of the i-th interferer from the mobile, the received power at a given mobile due to i-th interfering cell is proportional to $(D_i)^{-n}$ (the value of 'n' varies between 2 and 4 in urban cellular systems).

Let us take that the path loss exponent is same throughout the coverage area and the transmitted power be same, then SIR can be approximated as

$$\frac{S}{I} = \frac{R^{-n}}{\sum_{i=1}^N (D_i)^{-n}} \quad (3.15)$$

where the mobile is assumed to be located at R distance from the cell center. If we consider only the first layer of interfering cells and we assume that the interfering base stations are equidistant from the reference base station and the distance between the cell centers is 'D' then the above equation can be converted as

$$\frac{S}{I} = \frac{(D/R)^n}{i_n} = \frac{(\sqrt{3N})^n}{i_n} \quad (3.16)$$

than or equal to 18 dB. If we take $n=4$ the value of 'N' can be calculated as 6.49. Therefore minimum N is 7. The above equations are based on hexagonal geometry and the distances from the closest interfering cells can vary if different frequency reuse plans are used.

We can go for a more approximate calculation for co-channel SIR. This is the example of a 7 cell reuse case. The mobile is at a distance of D-R from 2 closest interfering cells and approximately $D+R/2$, D, $D-R/2$ and D+R distance from other interfering cells in the first tier. Taking $n = 4$ in the above equation, SIR can be approximately calculated as which is an approximate measure of the SIR. Subjective

tests performed on AMPS cellular system which uses FM and 30 kHz channels show that sufficient voice quality can be obtained by SIR being greater

$$\frac{S}{I} = \frac{R^{-4}}{2(D-R)^{-4} + (D+R)^{-4} + (D)^{-4} + (D+R/2)^{-4} + (D-R/2)^{-4}} \quad (3.17)$$

which can be rewritten in terms frequency reuse ratio Q as

$$\frac{S}{I} = \frac{1}{2(Q-1)^{-4} + (Q+1)^{-4} + (Q)^{-4} + (Q+1/2)^{-4} + (Q-1/2)^{-4}} \quad (3.18)$$

Using the value of N equal to 7 (this means Q = 4.6), the above expression yields that worst case SIR is 53.70 (17.3 dB). This shows that for a 7 cell reuse case the worst case SIR is slightly less than 18 dB. The worst case is when the mobile is at the corner of the cell i.e., on a vertex as shown in the Figure 3.6. Therefore N = 12 cluster size should be used. But this reduces the capacity by 7/12 times. Therefore, co-channel interference controls link performance, which in a way controls frequency reuse plan and the overall capacity of the cellular system. The effect of co-channel interference can be minimized by optimizing the frequency assignments of the base stations and their transmit powers. Tilting the base station antenna to limit the spread of the signals in the system can also be done.

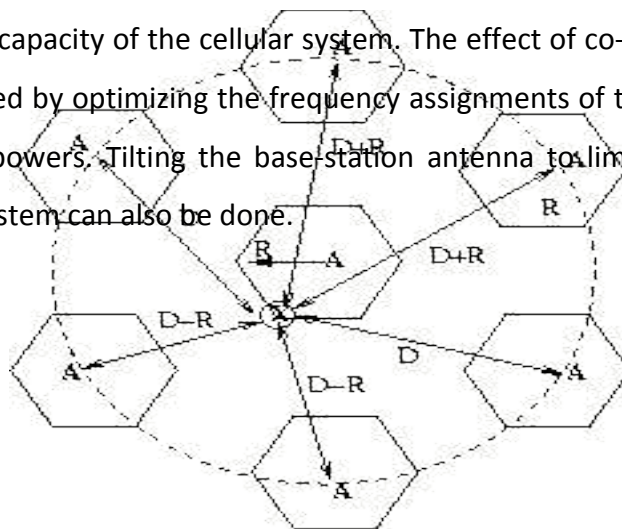


Figure 3.6: First tier of co-channel interfering cells

Adjacent Channel Interference (ACI)

This is a different type of interference which is caused by adjacent channels i.e. channels in adjacent cells. It is the signal impairment which occurs to one frequency due to presence of another signal on a nearby frequency. This occurs when imperfect receiver filters allow nearby frequencies to leak into the pass band. This problem is enhanced if the adjacent channel user is transmitting in a close range compared to the subscriber's receiver while the receiver attempts to receive a base station on the channel. This is called near-far effect. The more adjacent channels are packed into the channel block, the higher the spectral efficiency, provided that the performance degradation can be tolerated in the system link budget. This effect can also occur if a mobile close to a base station transmits on a channel close to one being used by a weak mobile. This problem might occur if the base station has problem in discriminating the mobile user from the "bleed over" caused by the close adjacent channel mobile.

Adjacent channel interference occurs more frequently in small cell clusters and heavily used cells. If the frequency separation between the channels is kept large this interference can be reduced to some extent. Thus assignment of channels is given such that they do not form a contiguous band of frequencies within a particular cell and frequency separation is maximized. Efficient assignment strategies are very much important in making the interference as less as possible. If the frequency factor is small then distance between the adjacent channels cannot put the interference level within tolerance limits. If a mobile is 10 times close to the base

station than other mobile and has energy spill out of its pass band, then SIR for weak mobile is approximately.

$$\frac{S}{I} = 10^{-n} \quad (3.19)$$

which can be easily found from the earlier SIR expressions. If $n = 4$, then SIR is -52 dB. Perfect base station filters are needed when close-in and distant users share the same cell. Practically, each base station receiver is preceded by a high Q cavity filter in order to remove adjacent channel interference. Power control is also very much important for the prolonging of the battery life for the subscriber unit but also reduces reverse channel SIR in the system. Power control is done such that each mobile transmits the lowest power required to maintain a good quality link on the reverse channel.

Power Control For Reducing Interference

In practical cellular radio and personal communication systems the power levels transmitted by every subscriber unit are under constant control by the serving base stations. This is done to ensure that each mobile transmits the smallest power necessary to maintain a good quality link on the reverse channel. Power control not only helps prolong battery life for subscriber unit, but also dramatically reduces the reverse channel S/I in the system.

Trunking and Grade of Service

In the previous sections, we have discussed the frequency reuse plan, the design trade-offs and also explored certain capacity expansion techniques like cell-splitting and sectoring. Now, we look at the relation between the number of radio channels a

cell contains and the number of users a cell can support. Cellular systems use the concept of trunking to accommodate a large number of users in a limited radio spectrum. It was found that a central office associated with say, 10,000 telephones requires about 50 million connections to connect every possible pair of users. However, a worst case maximum of 5000 connections need to be made among these telephones at any given instant of time, as against the possible 50 million connections. In fact, only a few hundreds of lines are needed owing to the relatively short duration of a call. This indicates that the resources are shared so that the number of lines is much smaller than the number of possible connections. A line that connects switching offices and that is shared among users on an as-needed basis is called a trunk.

The fact that the number of trunks needed to make connections between offices is much smaller than the maximum number that could be used suggests that at times there might not be sufficient facilities to allow a call to be completed. A call that cannot be completed owing to a lack of resources is said to be blocked. So one important to be answered in mobile cellular systems is: How many channels per cell are needed in a cellular telephone system to ensure a reasonably low probability that a call will be blocked?

In a trunked radio system, a channel is allotted on per call basis. The performance of a radio system can be estimated in a way by looking at how efficiently the calls are getting connected and also how they are being maintained at handoffs.

Some of the important factors to take into consideration are (i) Arrival statistics, (ii) Service statistics, (iii) Number of servers/channels.

Let us now consider the following assumptions for a bufferless system handling 'L' users as shown in Figure 3.11:

- (i) The number of users L is large when compared to 1.
- (ii) Arrival statistics is Poisson distributed with a mean parameter λ .

- (iii) Duration of a call is exponentially distributed with a mean rate μ_1 .
- (iv) Residence time of each user is exponentially distributed with a rate parameter μ_2
- (v) The channel holding rate therefore is exponentially distributed with a parameter $\mu = \mu_1 + \mu_2$.
- (vi) There is a total of 'J' number of channels ($J \leq L$).

To analyze such a system, let us recapitulate a queuing system in brief. Consider an M/M/m/m system which is an m-server loss system. The name M/M/m/m reflects

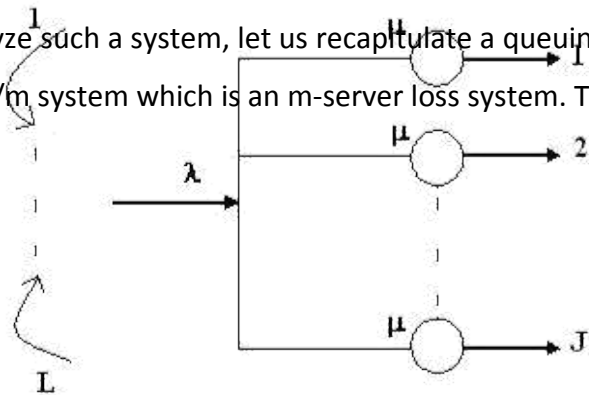


Figure 3.11: The bufferless J-channel trunked radio system

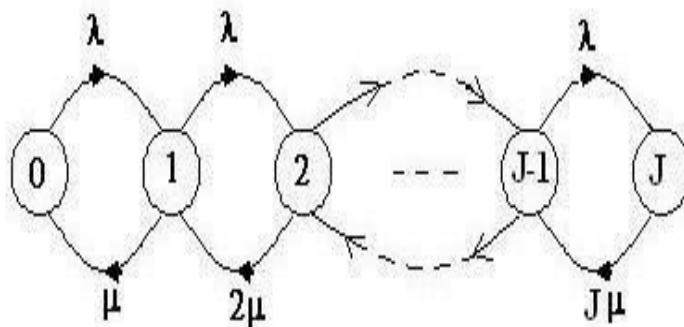
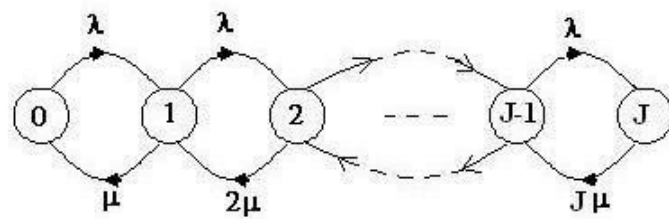


Figure 3.12: Discrete-time Markov chain for the M/M/J/J trunked radio system.



standard queuing theory nomenclature whereby:

- (i) the first letter indicates the nature of arrival process(e.g. M stands for memory-less which here means a Poisson process).
- (ii) the second letter indicates the nature of probability distribution of service times. (e.g M stands for exponential distribution). In all cases, successive inter arrival times and service times are assumed to be statistically independent of each other.
- (iii) the third letter indicates the number of servers.
- (iv) the last letter indicates that if an arrival finds all 'm' users to be busy, then it will not enter the system and is lost.

In view of the above, the bufferless system as shown in Figure 3.11 can be modeled as M/M/J/J system and the discrete-time Markov chain of this system is shown in Figure 3.12.

Trunking mainly exploits the statistical behavior of users so that a fixed number of channels can be used to accommodate a large, random user community. As the number of telephone lines decrease, it becomes more likely that all channels are busy for a particular user. As a result, the call gets rejected and in some systems, a queue may be used to hold the caller's request until a channel becomes available. In the telephone system context the term Grade of Service (GoS) is used to mean the probability that a user's request for service will be blocked because a required facility, such as a trunk or a cellular channel, is not available. For example, a GoS of 2 % implies that on the average a user might not be successful in placing a call on 2 out of every 100 attempts. In practice the blocking frequency varies with time. One would expect far more call attempts during business hours than during the middle of the night. Telephone operating companies maintain usage records and can identify a "busy hour", that is, the hour of the day during which there is the greatest demand for service. Typically, telephone systems are engineered to provide a specified grade of service during a specified busy hour.

User calling can be modeled statistically by two parameters: the average number of call requests per unit time λ_{user} and the average holding time H . The parameter λ_{user} is also called the average arrival rate, referring to the rate at which calls from a single user arrive. The average holding time is the average duration of a call. The product:

$$A_{user} = \lambda_{user} H \quad (3.26)$$

that is, the product of the average arrival rate and the average holding time—is called the offered traffic intensity or offered load. This quantity represents the average traffic that a user provides to the system. Offered traffic intensity is a quantity that is traditionally measured in Erlangs. One Erlang represents the amount of traffic intensity carried by a channel that is completely occupied. For example, a channel that is occupied for thirty minutes during an hour carries 0.5 Erlang of traffic.

Call arrivals or requests for service are modeled as a Poisson random process. It is based on the assumption that there is a large pool of users who do not cooperate in deciding when to place calls. Holding times are very well predicted using an exponential probability distribution. This implies that calls of long duration are much less frequent than short calls. If the traffic intensity offered by a single user is A_{user} , then the traffic intensity offered by N users is $A = NA_{user}$. The purpose of the statistical model is to relate the offered traffic intensity A , the grade of service P_b , and the number of channels or trunks C needed to maintain the desired grade of service.

Two models are widely used in traffic engineering to represent what happens when a call is blocked. The blocked calls cleared model assumes that when a channel or trunk is not available to service an arriving call, the call is cleared from the system. The second model is known as blocked calls delayed. In this model a call that cannot be serviced is placed on a queue and will be serviced when a channel or trunk becomes available.

Use of the blocked-calls-cleared statistical model leads to the Erlang B formula that relates offered traffic intensity A , grade of service P_b , and number of channels

K. The Erlang B formula is:

$$P_b = \frac{A^K / K!}{\sum_{n=0}^K A^n / n!} \quad (3.27)$$

When the blocked-calls-delayed model is used, the "grade of service" refers to the probability that a call will be delayed. In this case the statistical model leads to the Erlang C formula,

$$P[\text{delay}] = \frac{A^K / [(K - A)(K - 1)!]}{A^K / [(K - A)(K - 1)!] + \sum_{n=0}^{K-1} A^n / n!} \quad (3.28)$$

Improving Coverage and Capacity in Cellular Systems

Previously, we have seen that the frequency reuse technique in cellular systems allows for almost boundless expansion of geographical area and the number of mobile system users who could be accommodated. In designing a cellular layout, the two parameters which are of great significance are the cell radius R and the cluster size N , and we have also seen that co-channel cell distance $D = \sqrt{3NR}$. In the following, a brief description of the design trade-off is given, in which the above two parameters play a crucial role.

The cell radius governs both the geographical area covered by a cell and also the number of subscribers who can be serviced, given the subscriber density. It is easy to see that the cell radius must be as large as possible. This is because, every cell requires an investment

in a tower, land on which the tower is placed, and radio transmission equipment and so a large cell size minimizes the cost per subscriber. Eventually, the cell radius is determined by the requirement that adequate signal to noise ratio be maintained over the coverage area. The SNR is determined by several factors such as the antenna height, transmitter power, receiver noise figure etc. Given a cell radius R and a cluster size N , the geographic area covered by a cluster is

$$A_{cluster} = NA_{cell} = N3^{\sqrt{3}}R^2/2. \quad (3.20)$$

If the total serviced area is A_{total} , then the number of clusters M that could be accommodated is given by

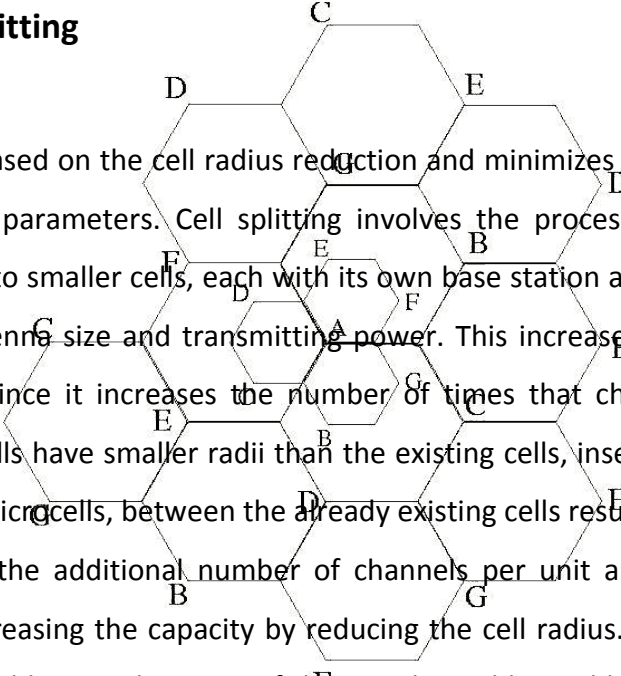
$$M = A_{total}/A_{cluster} = A_{total}/(N3^{\sqrt{3}}R^2/2). \quad (3.21)$$

Note that all of the available channels N , are reused in every cluster. Hence, to make the maximum number of channels available to subscribers, the number of clusters M should be large, which, by Equation (3.21), shows that the cell radius should be small. However, cell radius is determined by a trade-off: R should be as large as possible to minimize the cost of the installation per subscriber, but R should be as small as possible to maximize the number of customers that the system can accommodate. Now, if the cell radius R is fixed, then the number of clusters could be maximized by minimizing the size of a cluster N . We have seen earlier that the size of a cluster depends on the frequency reuse ratio Q . Hence, in determining the value of N , another trade-off is encountered in that N must be small to accommodate large number of subscribers, but should be sufficiently large so as to minimize the interference effects.

Now, we focus on the issues regarding system expansion. The history of cellular phones has been characterized by a rapid growth and expansion in cell subscribers. Though a cellular system can be expanded by simply adding cells to the geographical area, the way in which user density can be increased is also important to look at. This is because it is not always possible to counter the increasing demand for cellular systems just by increasing the geographical coverage area due to the limitations in obtaining new land with suitable requirements. We discuss here two methods for dealing with an increasing subscriber density: Cell Splitting and Sectoring. The other method, microcell zone concept can be treated as enhancing the QoS in a cellular system.

The basic idea of adopting the cellular approach is to allow space for the growth of mobile users. When a new system is deployed, the demand for it is fairly low and users are assumed to be uniformly distributed over the service area. However, as new users subscribe to the cellular service, the demand for channels may begin to exceed the capacity of some base stations. As discussed previously, the number of channels available to customers (equivalently, the channel density per square kilometer) could be increased by decreasing the cluster size. However, once a system has been initially deployed, a system-wide reduction in cluster size may not be necessary since user density does not grow uniformly in all parts of the geographical area. It might be that an increase in channel density is required only in specific parts of the system to support an increased demand in those areas. Cell-splitting is a technique which has the capability to add new smaller cells in specific areas of the system.

Cell-Splitting



Cell Splitting is based on the cell radius reduction and minimizes the need to modify the existing cell parameters. Cell splitting involves the process of sub-dividing a congested cell into smaller cells, each with its own base station and a corresponding reduction in antenna size and transmitting power. This increases the capacity of a cellular system since it increases the number of times that channels are reused. Since the new cells have smaller radii than the existing cells, inserting these smaller cells, known as microcells, between the already existing cells results in an increase of capacity due to the additional number of channels per unit area. There are few challenges in increasing the capacity by reducing the cell radius. Clearly, if cells are small, there would have to be more of them and so additional base stations will be needed in the system. The challenge in this case is to introduce the new base stations without the need to move the already existing base station towers. The other challenge is to meet the generally increasing demand that may vary quite rapidly between geographical areas of the system. For instance, a city may have highly populated areas and so the demand must be supported by cells with the smallest radius. The radius of cells will generally increase as we move from urban to sub urban areas, because the user density decreases on moving towards sub-urban areas. The key factor is to add as minimum number of smaller cells as possible wherever an increase in demand occurs. The gradual addition of the smaller cells implies that, at least for a time, the cellular system operates with cells of more than one size.

Figure 3.7: Splitting of congested seven-cell clusters.

Figure 3.7 shows a cellular layout with seven-cell clusters. Consider that the cells in the center of the diagram are becoming congested, and cell A in the center has reached its maximum capacity. Figure also shows how the smaller cells are being superimposed on the original layout. The new smaller cells have half the cell radius of the original cells. At half the radius, the new cells will have one-fourth of the area and will consequently need to support one-fourth the number of subscribers. Notice that one of the new smaller cells lies in the center of each of the larger cells. If we assume that base stations are located in the cell centers, this allows the original base stations to be maintained even in the new system layout. However, new base stations will have to be added for new cells that do not lie in the center of the larger cells. The organization of cells into clusters is independent of the cell radius, so that the cluster size can be the same in the small-cell layout as it was in the large-cell layout. Also the signal-to-interference ratio is determined by cluster size and not by cell radius. Consequently, if the cluster size is maintained, the signal-to-interference ratio will be the same after cell splitting as it was before. If the entire system is

replaced with new half-radius cells, and the cluster size is maintained, the number of channels per cell will be exactly as it was before, and the number of subscribers per cell will have been reduced.

When the cell radius is reduced by a factor, it is also desirable to reduce the transmitted power. The transmit power of the new cells with radius half that of the old cells can be found by examining the received power P_R at the new and old cell boundaries and setting them equal. This is necessary to maintain the same frequency re-use plan in the new cell layout as well. Assume that P_{T1} and P_{T2} are the transmit powers of the larger and smaller base stations respectively. Then, assuming a path loss index $n=4$, we have power received at old cell boundary = P_{T1}/R^4 and the power received at new cell boundary = $P_{T2}/(R/2)^4$. On equating the two received powers, we get $P_{T2} = P_{T1} / 16$. In other words, the transmit power must be reduced by 12 dB in order to maintain the same S/I with the new system lay-out.

At the beginning of this channel splitting process, there would be fewer channels in the smaller power groups. As the demand increases, more and more channels need to be accommodated and hence the splitting process continues until all the larger cells have been replaced by the smaller cells, at which point splitting is complete within the region and the entire system is rescaled to have a smaller radius per cell. If a cellular layout is replaced entirely by a new layout with a smaller cell radius, the signal-to-interference ratio will not change, provided the cluster size does not change. Some special care must be taken, however, to avoid co-channel interference when both large and small cell radii coexist. It turns out that the only way to avoid interference between the large-cell and small-cell systems is to assign entirely different sets of channels to the two systems. So, when two sizes of cells coexist in a system, channels in the old cell must be broken down into two groups, one that corresponds to larger cell reuse requirements and the other which corresponds to the smaller cell reuse requirements. The larger cell is usually dedicated to high

speed users as in the umbrella cell approach so as to minimize the number of hand-offs.

Sectoring

Sectoring is basically a technique which can increase the SIR without necessitating an increase in the cluster size. Till now, it has been assumed that the base station is located in the center of a cell and radiates uniformly in all the directions behaving as an omni-directional antenna. However it has been found that the co-channel interference in a cellular system may be decreased by replacing a single omni-directional antenna at the base station by several directional antennas, each radiating within a specified sector. In the Figure 3.8, a cell is shown which has been split into three 120° sectors. The base station feeds three 120° directional antennas, each of which radiates into one of the three sectors. The channel set serving this cell has also been divided, so that each sector is assigned one-third of the available number cell of channels. This technique for reducing co-channel interference wherein by using suitable

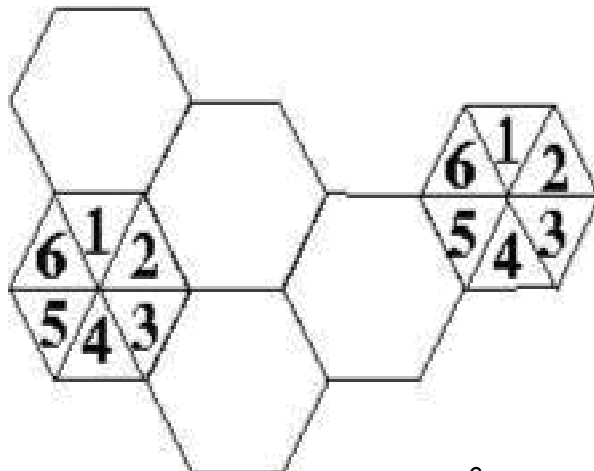


Figure 3.9: A seven-cell cluster with 60° sectors.

directional antennas, a given cell would receive interference and transmit with a fraction of available co-channel cells is called 'sectoring'. In a seven-cell-cluster layout with 120° sectored cells, it can be easily understood that the mobile units in a particular sector of the center cell will receive co-channel interference from only two of the first-tier co-channel base stations, rather than from all six. Likewise, the base station in the center cell will receive co-channel interference from mobile units in only two of the co-channel cells. Hence the signal to interference ratio is now modified to

$$\frac{S}{I} = \left(\frac{\sqrt{3N}}{2} \right)^n \quad (3.22)$$

where the denominator has been reduced from 6 to 2 to account for the reduced number of interfering sources. Now, the signal to interference ratio for a seven-cell cluster layout using 120° sectored antennas can be found from equation (3.24) to be 23.4 dB which is a significant improvement over the Omni-directional case where the worst-case S/I is found to be 17 dB (assuming a path-loss exponent, n=4). Some cellular systems divide the cells into 60° sectors. Similar analysis can be performed on them as well.

Microcell Zone Concept

The increased number of handoffs required when sectoring is employed results in an increased load on the switching and control link elements of the mobile system. To overcome this problem, a new microcell zone concept has been proposed. As shown in Figure 3.10, this scheme has a cell divided into three microcell zones, with each of the three zone sites connected to the base station and sharing the same radio equipment. It is necessary to note that all the microcell zones, within a cell, use the same frequency used by that cell; that is no handovers occur between microcells. Thus when a mobile user moves between two microcell zones of the cell, the BS

simply switches the channel to a different zone site and no physical re-allotment of channel takes place.

Locating the mobile unit within the cell: An active mobile unit sends a signal to all zone sites, which in turn send a signal to the BS. A zone selector at the BS uses that signal to select a suitable zone to serve the mobile unit - choosing the zone with the strongest signal.

Base Station Signals: When a call is made to a cellular phone, the system already knows the cell location of that phone. The base station of that cell knows in which zone, within that cell, the cellular phone is located. Therefore when it receives the signal, the base station transmits it to the suitable zone site. The zone site receives the cellular signal from the base station and transmits that signal to the mobile phone after amplification. By confining the power transmitted to the mobile phone, co-channel interference is reduced between the zones and the capacity of system is increased.

Benefits of the micro-cell zone concept: 1) Interference is reduced in this case as compared to the scheme in which the cell size is reduced.

2) Handoffs are reduced (also compared to decreasing the cell size) since the micro-cells within the cell operate at the same frequency; no handover occurs when the mobile unit moves between the microcells.

3) Size of the zone apparatus is small. The zone site equipment being small can be mounted on the side of a building or on poles.

4) System capacity is increased. The new microcell knows where to locate the mobile unit in a particular zone of the cell and deliver the power to that zone. Since

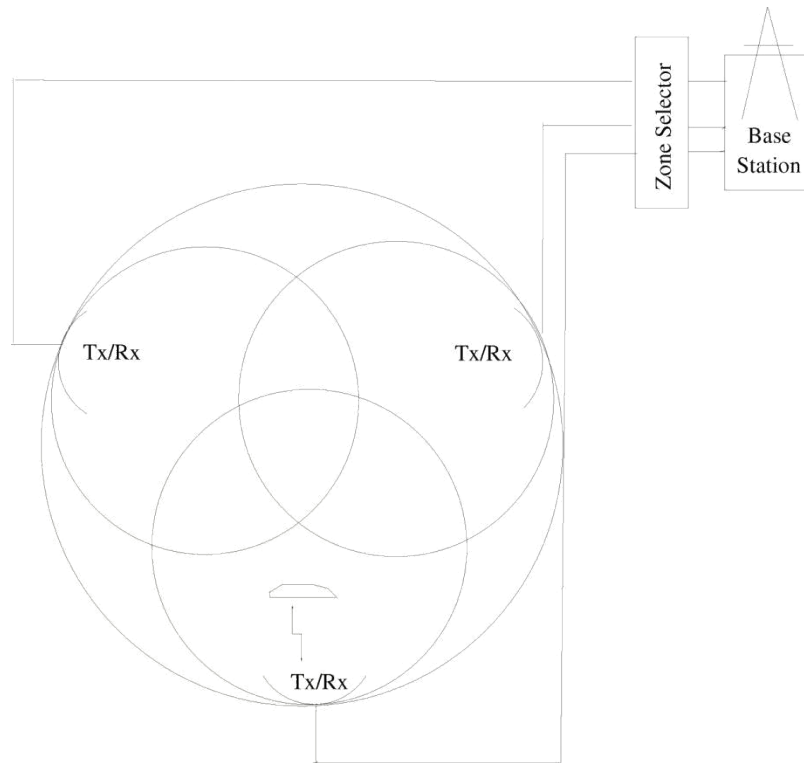


Figure 3.10: The micro-cell zone concept

the signal power is reduced, the microcells can be closer and result in an increased system capacity. However, in a microcellular system, the transmitted power to a mobile phone within a microcell has to be precise; too much power results in interference between microcells, while with too little power the signal might not reach the mobile phone. This is a drawback of microcellular systems, since a change in the surrounding (a new building, say, within a microcell) will require a change of the transmission power.

Unit -2 Mobile Radio Propagation:

Large-Scale Path Loss

Introduction

There are two basic ways of transmitting an electro-magnetic (EM) signal, through a guided medium or through an unguided medium. Guided mediums such as coaxial cables and fiber optic cables, are far less hostile toward the information carrying EM signal than the wireless or the unguided medium. It presents challenges and conditions which are unique for this kind of transmissions. A signal, as it travels through the wireless channel, undergoes many kinds of propagation effects such as reflection, diffraction and scattering, due to the presence of buildings, mountains and other such obstructions. Reflection occurs when the EM waves impinge on objects which are much greater than the wavelength of the traveling wave. Diffraction is a phenomena occurring when the wave interacts with a surface having sharp irregularities. Scattering occurs when the medium through the wave is traveling contains objects which are much smaller than the wavelength of the EM wave. These varied phenomena's lead to large scale and small scale propagation losses. Due to the inherent randomness associated with such channels they are best described with the help of statistical models. Models which predict the mean signal strength for arbitrary transmitter receiver distances are termed as large scale propagation models. These are termed so because they predict the average signal strength for large Tx-Rx separations, typically for hundreds of kilometers.

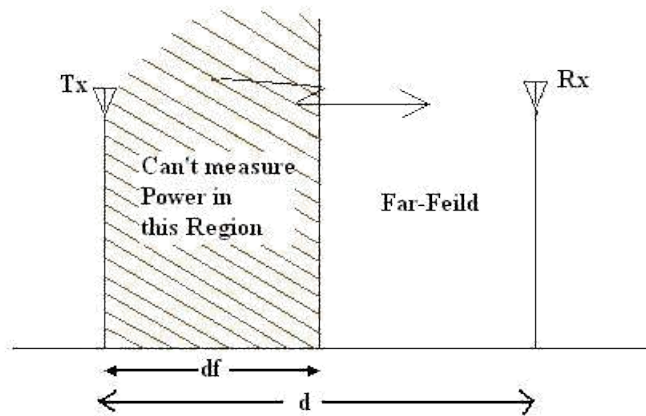


Figure 4.1: Free space propagation model, showing the near and far fields.

Free Space Propagation Model

Although EM signals when traveling through wireless channels experience fading effects due to various effects, but in some cases the transmission is with a direct line of sight such as in satellite communication. Free space model predicts that the received power decays as negative square root of the distance. Friis free space equation is given by

$$P_r(d) = \frac{P_t t_t t_r \lambda^2}{(4\pi)^2 d^2 L} \quad (4.1)$$

where P_t is the transmitted power, $P_r(d)$ is the received power, t_t is the transmitter antenna gain, t_r is the receiver antenna gain, d is the Tx-Rx separation and L is the system loss factor depended upon line attenuation, filter losses and antenna losses and not related to propagation. The gain of the antenna is related to the effective aperture of the antenna which in turn is dependent upon the physical size of the antenna as given below

$$t_t = 4\pi A_e / \lambda^2. \quad (4.2)$$

The path loss, representing the attenuation suffered by the signal as it travels through the wireless channel is given by the difference of the transmitted and received power in dB and is expressed as:

$$PL(dB) = 10 \log P_t / P_r. \quad (4.3)$$

The fields of an antenna can broadly be classified in two regions, the far field and the near field. It is in the far field that the propagating waves act as plane waves and the power decays inversely with distance. The far field region is also termed as Fraunhofer region and the Friis equation holds in this region. Hence, the Friis equation is used only beyond the far field distance, d_f , which is dependent upon the largest dimension of the antenna as

$$d_f = 2D^2/\lambda. \quad (4.4)$$

Also we can see that the Friis equation is not defined for $d=0$. For this reason, we use a close in distance, d_0 , as a reference point. The power received, $Pr(d)$, is then given by:

$$Pr(d) = Pr(d_0)(d_0/d)^2. \quad (4.5)$$

Ex. 1: Find the far field distance for a circular antenna with maximum dimension of 1 m and operating frequency of 900 MHz.

Solution: Since the operating frequency $f = 900$ Mhz, the wavelength

$$\lambda = \frac{3 \times 10^8 \text{ m/s}}{900 \times 10^6 \text{ Hz}}$$

. Thus, with the largest dimension of the antenna, $D=1\text{m}$, the far field distance is

$$d_f = \frac{2D^2}{\lambda} = \frac{2(1)^2}{0.33} = 6\text{m}$$

Ex. 2: A unit gain antenna with a maximum dimension of 1 m produces 50 W power at 900 MHz. Find (i) the transmit power in dBm and dB, (ii) the received power at a free space distance of 5 m and 100 m. Solution:

(i) Tx power = $10\log(50) = 17 \text{ dB} = (17+30) \text{ dBm} = 47 \text{ dBm}$

(ii) $d_f = \frac{2 \times D^2}{\lambda} = \frac{2 \times 1^2}{1/3} = 6\text{m}$

Thus the received power at 5 m can not be calculated using free space distance formula.

At 100 m ,

$$P_R = \frac{P_T G_T G_R \lambda^2}{4\pi d^2} = \frac{50 \times 1 \times (1/3)^2}{4\pi 100^2}$$

3.3 Relating Power to Electric Field

3.3 Relating Power to Electric Field

The free space path loss model of Section 3.2 is readily derived from first

3.3 Relating Power to Electric Field

The free space path loss model of Section 3.2 is readily derived from first principles. It can be proven that any radiating structure produces electric and magnetic fields [Gri87], [Kra50]. Consider a small linear radiator of length L , that is placed coincident with the z -axis and has its center at the origin, as shown in Figure 3.2.

3.3 Relating Power to Electric Field

The free space path loss model of Section 3.2 is readily derived from first principles. It can be proven that any radiating structure produces electric and magnetic fields [Gri87], [Kra50]. Consider a small linear radiator of length L , that is placed coincident with the z -axis and has its center at the origin, as shown in Figure 3.2.

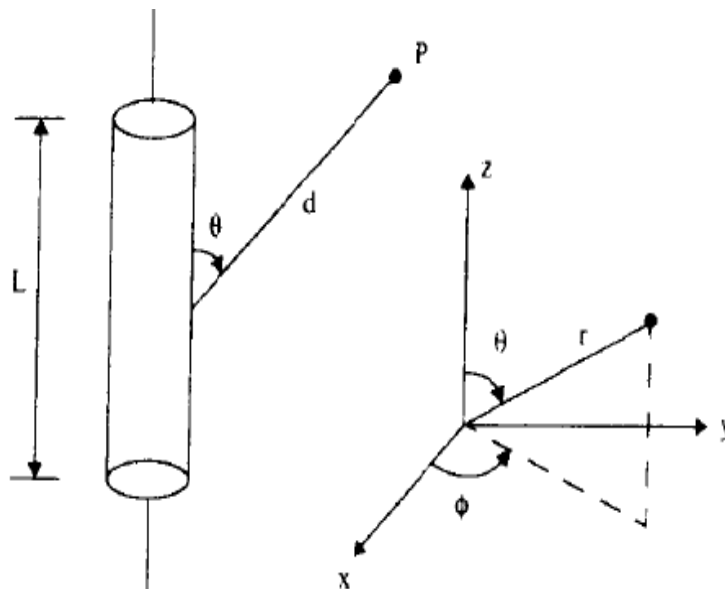


Figure 3.2

Illustration of a linear radiator of length L ($L \ll \lambda$), carrying a current of amplitude i_0 and making an angle θ with a point, at distance d .

If a current flows through such an antenna, it launches electric and magnetic fields that can be expressed as

$$E_r = \frac{i_0 L \cos \theta}{2\pi\epsilon_0 c} \left\{ \frac{1}{d^2} + \frac{c}{j\omega_c d^3} \right\} e^{j\omega_c(t-d/c)} \quad (3.10)$$

$$E_\theta = \frac{i_0 L \sin \theta}{4\pi\epsilon_0 c^2} \left\{ \frac{j\omega_c}{d} + \frac{c}{d^2} + \frac{c^2}{j\omega_c d^3} \right\} e^{-j\omega_c(t-d/c)} \quad (3.11)$$

$$H_\phi = \frac{i_0 L \sin \theta}{4\pi c} \left\{ \frac{j\omega_c}{d} + \frac{c}{d^2} \right\} e^{j\omega_c(t-d/c)} \quad (3.12)$$

with $E_\phi = H_r = H_\theta = 0$. In the above equations, all $1/d$ terms represent the radiation field component, all $1/d^2$ terms represent the induction field component, and all $1/d^3$ terms represent the electrostatic field component. As seen from equations (3.10) to (3.12), the electrostatic and inductive fields decay much faster with distance than the radiation field. At regions far away from the transmitter (far-field region), the electrostatic and inductive fields become negligible and only the radiated field components of E_θ and H_ϕ need be considered.

In free space, the *power flux density* P_d (expressed in W/m^2) is given by

$$P_d = \frac{EIRP}{4\pi d^2} = \frac{P_t G_t}{4\pi d^2} = \frac{E^2}{R_{fs}} = \frac{E^2}{\eta} \text{ W/m}^2 \quad (3.13)$$

where R_{fs} is the intrinsic impedance of free space given by $\eta = 120\pi \Omega$ (377Ω). Thus, the power flux density is

$$P_d = \frac{|E|^2}{377\Omega} \text{ W/m}^2 \quad (3.14)$$

where $|E|$ represents the magnitude of the radiating portion of the electric field in the far field. Figure 3.3a illustrates how the power flux density disperses in free space from an isotropic point source. P_d may be thought of as the *EIRP* divided by the surface area of a sphere with radius d . The power received at distance d , $P_r(d)$, is given by the power flux density times the effective aperture of the receiver antenna, and can be related to the electric field using equations (3.1), (3.2), (3.13), and (3.14).

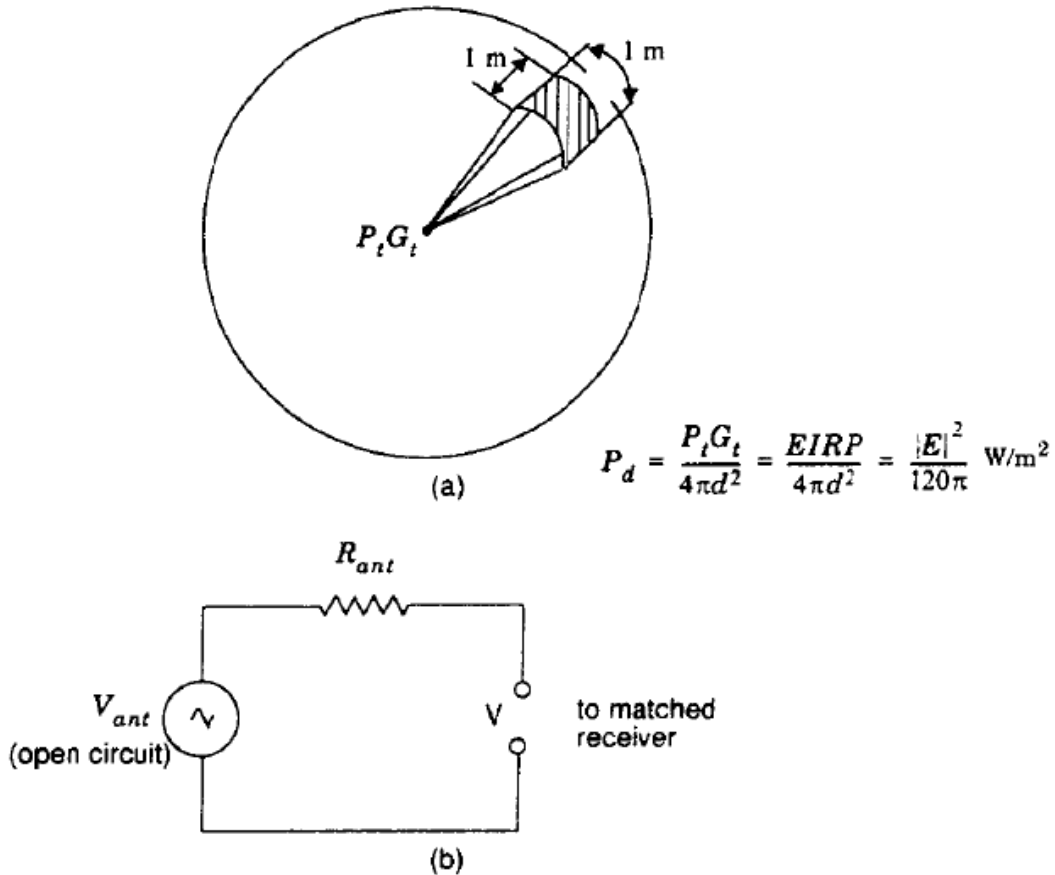


Figure 3.3
 (a) Power flux density at a distance d from a point source.
 (b) Model for voltage applied to the input of a receiver.

$$P_r(d) = P_d A_e = \frac{|E|^2}{120\pi} A_e = \frac{P_t G_t G_r \lambda^2}{(4\pi)^2 d^2} \text{ Watts} \quad (3.15)$$

Equation (3.15) relates electric field (with units of V/m) to received power (with units of watts), and is identical to equation (3.1) with $L = 1$.

Often it is useful to relate the received power level to a receiver input voltage, as well as to an induced E-field at the receiver antenna. If the receiver

antenna is modeled as a matched resistive load to the receiver, then the received antenna will induce an rms voltage into the receiver which is half of the open circuit voltage at the antenna. Thus, if V is the rms voltage at the input of a receiver (measured by a high impedance voltmeter), and R_{ant} is the resistance of the matched receiver, the received power is given by

$$P_r(d) = \frac{V^2}{R_{ant}} = \frac{[V_{ant}/2]^2}{R_{ant}} = \frac{V_{ant}^2}{4R_{ant}} \quad (3.16)$$

Through equations (3.14) to (3.16), it is possible to relate the received power to the received E-field or the open circuit rms voltage at the receiver antenna terminals. Figure 3.3b illustrates an equivalent circuit model. Note $V_{ant} = V$ when there is no load.

Basic Methods of Propagation

Reflection, diffraction and scattering are the three fundamental phenomena that cause signal propagation in a mobile communication system, apart from LoS communication. The most important parameter, predicted by propagation models based on above three phenomena, is the received power. The physics of the above phenomena may also be used to describe small scale fading and multipath propagation. The following subsections give an outline of these phenomena.

Reflection

Reflection occurs when an electromagnetic wave falls on an object, which has very large dimensions as compared to the wavelength of the propagating wave. For example, such objects can be the earth, buildings and walls. When a radio wave falls on another medium having different electrical properties, a part of it is transmitted into it, while some energy is reflected back. Let us see some special cases. If the medium on which the e.m. wave is incident is a dielectric, some energy is reflected back and some energy is transmitted. If the medium is a perfect conductor, all energy is reflected back to the first medium. The amount of energy that is reflected back depends on the polarization of the e.m. wave.

Another particular case of interest arises in parallel polarization, when no reflection occurs in the medium of origin. This would occur, when the incident

angle would be such that the reflection coefficient is equal to zero. This angle is the Brewster's angle. By applying laws of electro-magnetics, it is found to be

$$\sin(\theta_B) = \frac{s_1}{s_1 + s_2} \quad (4.6)$$

Further, considering perfect conductors, the electric field inside the conductor is always zero. Hence all energy is reflected back. Boundary conditions require that

$$\theta_i = \theta_r \quad (4.7)$$

and

$$E_i = E_r \quad (4.8)$$

for vertical polarization, and

$$E_i = -E_r \quad (4.9)$$

for horizontal polarization.

3.5.1 Reflection from Dielectrics

Figure 3.4 shows an electromagnetic wave incident at an angle θ_i with the plane of the boundary between two dielectric media. As shown in the figure, part of the energy is reflected back to the first media at an angle θ_r , and part of the energy is transmitted (refracted) into the second media at an angle θ_t . The nature of reflection varies with the direction of polarization of the E-field. The behavior for arbitrary directions of polarization can be studied by considering the two distinct cases shown in Figure 3.4. The *plane of incidence* is defined as the plane containing the incident, reflected, and transmitted rays [Ram65]. In Figure 3.4a, the E-field polarization is parallel with the plane of incidence (that is, the E-field has a vertical polarization, or normal component, with respect to the reflecting surface) and in Figure 3.4b, the E-field polarization is perpendicular to the plane of incidence (that is, the incident E-field is pointing out of the page towards the reader, and is perpendicular to the page and parallel to the reflecting surface).

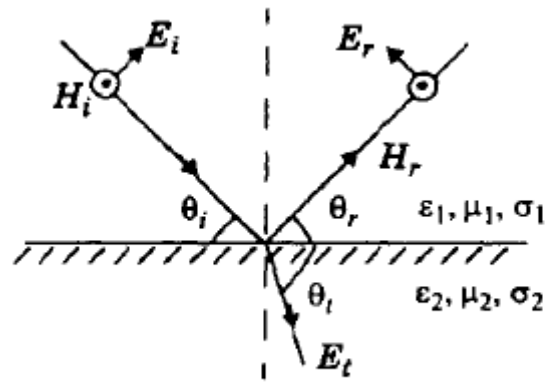
In Figure 3.4, the subscripts i , r , t refer to the incident, reflected, and transmitted fields, respectively. Parameters ϵ_1 , μ_1 , σ_1 , and ϵ_2 , μ_2 , σ_2 represent the permittivity, permeability, and conductance of the two media, respectively. Often, the dielectric constant of a perfect (lossless) dielectric is related to a relative value of permittivity, ϵ_r , such that $\epsilon = \epsilon_0 \epsilon_r$, where ϵ_0 is a constant given by 8.85×10^{-12} F/m. If a dielectric material is lossy, it will absorb power and may be described by a complex dielectric constant given by

$$\epsilon = \epsilon_0 \epsilon_r - j\epsilon' \quad (3.17)$$

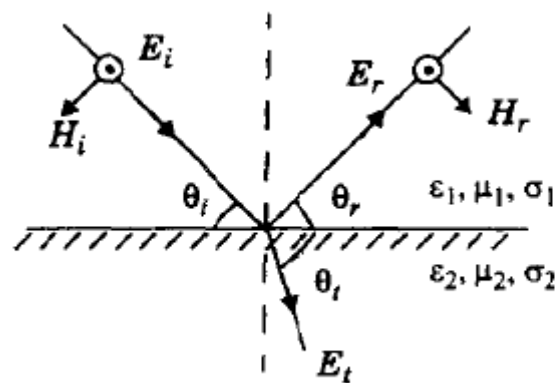
where,

$$\epsilon' = \frac{\sigma}{2\pi f} \quad (3.18)$$

and σ is the conductivity of the material measured in Siemens/meter. The terms ϵ_r and σ are generally insensitive to operating frequency when the material is a good conductor ($f < \sigma / (\epsilon_0 \epsilon_r)$). For lossy dielectrics, ϵ_0 and ϵ_r are generally constant with frequency, but σ may be sensitive to the operating frequency, as shown in Table 3.1. Electrical properties of a wide range of materials were characterized over a large frequency range by Von Hippel [Von54].



(a) E-field in the plane of incidence



(b) E-field normal to the plane of incidence

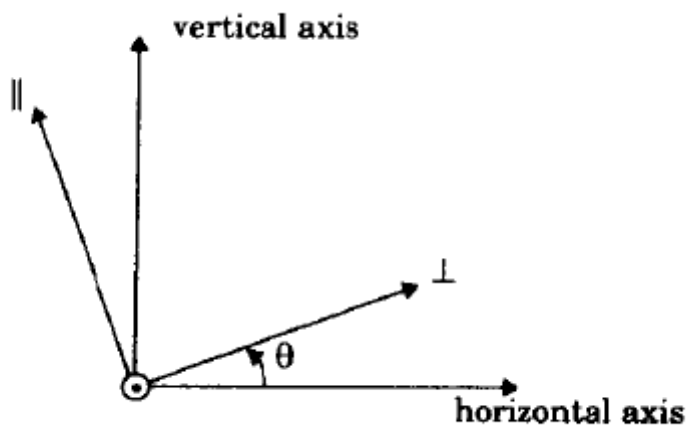
Figure 3.4

Geometry for calculating the reflection coefficients between two dielectrics.

Table 3.1 Material Parameters at Various Frequencies

Material	Relative Permittivity ϵ_r	Conductivity σ (s/m)	Frequency (MHz)
Poor Ground	4	0.001	100
Typical Ground	15	0.005	100
Good Ground	25	0.02	100
Sea Water	81	5.0	100
Fresh Water	81	0.001	100
Brick	4.44	0.001	4000
Limestone	7.51	0.028	4000
Glass, Corning 707	4	0.00000018	1
Glass, Corning 707	4	0.000027	100
Glass, Corning 707	4	0.005	10000

Because of superposition, only two orthogonal polarizations need be considered to solve general reflection problems. The reflection coefficients for the two cases of parallel and perpendicular E-field polarization at the boundary of two dielectrics are given by



$$\Gamma_{\parallel} = \frac{E_r}{E_i} = \frac{\eta_2 \sin \theta_t - \eta_1 \sin \theta_i}{\eta_2 \sin \theta_t + \eta_1 \sin \theta_i} \quad (\text{E-field in plane of incidence}) \quad (3.19)$$

$$\Gamma_{\perp} = \frac{E_r}{E_i} = \frac{\eta_2 \sin \theta_i - \eta_1 \sin \theta_t}{\eta_2 \sin \theta_i + \eta_1 \sin \theta_t} \quad (\text{E-field not in plane of incidence}) \quad (3.20)$$

where η_i is the intrinsic impedance of the i th medium ($i = 1, 2$), and is given by $\sqrt{\mu_i/\epsilon_i}$, the ratio of electric to magnetic field for a uniform plane wave in the particular medium. The velocity of an electromagnetic wave is given by $1/(\sqrt{\mu\epsilon})$, and the boundary conditions at the surface of incidence obey Snell's Law which, referring to Figure 3.4, is given by

$$\sqrt{\mu_1 \epsilon_1} \sin(90 - \theta_i) = \sqrt{\mu_2 \epsilon_2} \sin(90 - \theta_t) \quad (3.21)$$

The boundary conditions from Maxwell's equations are used to derive equations (3.19) and (3.20) as well as equations (3.22), (3.23.a), and (3.23.b).

$$\theta_i = \theta_r \quad (3.22)$$

and

$$E_r = \Gamma E_i \quad (3.23.a)$$

$$E_t = (1 + \Gamma) E_i \quad (3.23.b)$$

where Γ is either Γ_{\parallel} or Γ_{\perp} , depending on polarization.

For the case when the first medium is free space and $\mu_1 = \mu_2$, the reflection coefficients for the two cases of vertical and horizontal polarization can be simplified to

$$\Gamma_{\parallel} = \frac{-\epsilon_r \sin \theta_i + \sqrt{\epsilon_r - \cos^2 \theta_i}}{\epsilon_r \sin \theta_i + \sqrt{\epsilon_r - \cos^2 \theta_i}} \quad (3.24)$$

and

$$\Gamma_{\perp} = \frac{\sin \theta_i - \sqrt{\epsilon_r - \cos^2 \theta_i}}{\sin \theta_i + \sqrt{\epsilon_r - \cos^2 \theta_i}} \quad (3.25)$$

For the case of elliptical polarized waves, the wave may be broken down (depolarized) into its vertical and horizontal E-field components, and superposition may be applied to determine transmitted and reflected waves. In the general case of reflection or transmission, the horizontal and vertical axes of the spatial coordinates may not coincide with the perpendicular and parallel axes of the propagating waves. An angle θ measured counter-clockwise from the horizontal axis is defined as shown in Figure 3.5 for a propagating wave out of the page (towards the reader) [Stu93]. The vertical and horizontal field components at a dielectric boundary may be related by

3.5.2 Brewster Angle

The *Brewster angle* is the angle at which no reflection occurs in the medium of origin. It occurs when the incident angle θ_B is such that the reflection coefficient Γ_{\parallel} is equal to zero (see Figure 3.6). The Brewster angle is given by the value of θ_B which satisfies

$$\sin(\theta_B) = \frac{\sqrt{\epsilon_1}}{\sqrt{\epsilon_1 + \epsilon_2}} \quad (3.27)$$

For the case when the first medium is free space and the second medium has a relative permittivity ϵ_r , equation (3.27) can be expressed as

$$\sin(\theta_B) = \frac{\sqrt{\epsilon_r - 1}}{\sqrt{\epsilon_r + 1}} \quad (3.28)$$

Note that the Brewster angle occurs only for vertical (i.e. parallel) polarization.

3.5.3 Reflection from Perfect Conductors

Since electromagnetic energy cannot pass through a perfect conductor a plane wave incident on a conductor has all of its energy reflected. As the electric field at the surface of the conductor must be equal to zero at all times in order to obey Maxwell's equations, the reflected wave must be equal in magnitude to the incident wave. For the case when E-field polarization is in the plane of incidence, the boundary conditions require that [Ram65]

$$\theta_i = \theta_r \quad (3.29)$$

and

$$E_i = E_r \quad (\text{E-field in plane of incidence}) \quad (3.30)$$

Similarly, for the case when the E-field is horizontally polarized, the boundary conditions require that

$$\theta_i = \theta_r \quad (3.31)$$

and

$$E_i = -E_r \quad (\text{E-field not in plane of incidence}) \quad (3.32)$$

Referring to equations (3.29) to (3.32), we see that for a perfect conductor, $\Gamma_{\parallel} = 1$, and $\Gamma_{\perp} = -1$, regardless of incident angle. Elliptical polarized waves may be analyzed by using superposition, as shown in Figure 3.5 and equation (3.26).

Two Ray Reflection Model

Interaction of EM waves with materials having different electrical properties than the material through which the wave is traveling leads to transmitting of energy through the medium and reflection of energy back in the medium of propagation. The amount of energy reflected to the amount of energy incidented is represented by Fresnel reflection coefficient Γ , which depends upon the wave polarization, angle of incidence and frequency of the wave. For example, as the EM waves can not pass through conductors, all the energy is reflected back with angle of incidence equal to the angle of reflection and reflection coefficient $\Gamma = -1$. In general, for parallel and perpendicular polarizations, Γ is given by:

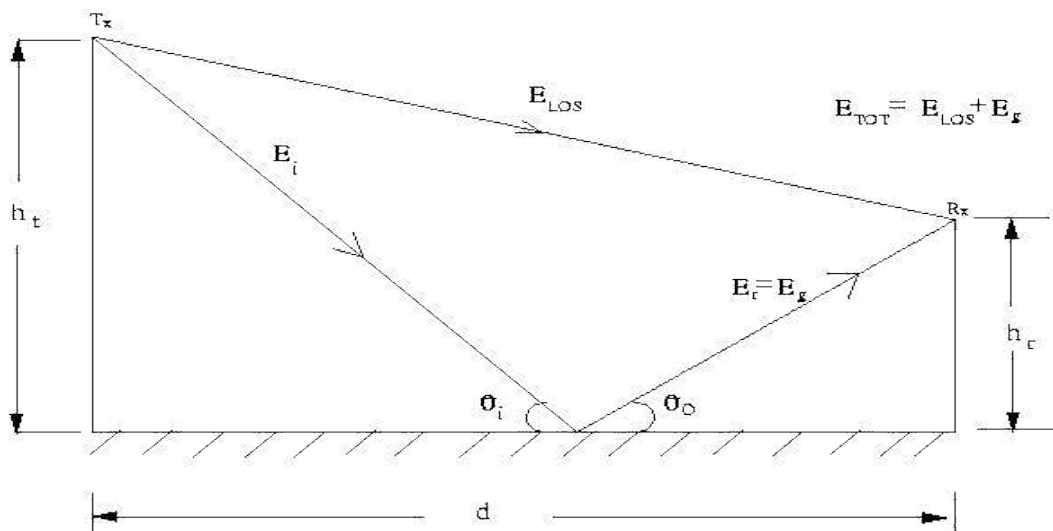


Figure 4.2: Two-ray reflection model.

which agrees very well for large walls made of limestone. The equivalent reflection coefficient is given by,

$$\Gamma_{rough} = \rho S \Gamma. \quad (4.13)$$

$$\Gamma_{||} = E_r/E_i = \eta_2 \sin \vartheta_t - \eta_1 \sin \vartheta_i / \eta_2 \sin \vartheta_t + \eta_1 \sin \vartheta_i \quad (4.14)$$

$$\Gamma_{\perp} = E_r/E_i = \eta_2 \sin \vartheta_i - \eta_1 \sin \vartheta_t / \eta_2 \sin \vartheta_i + \eta_1 \sin \vartheta_t.$$

Seldom in communication systems we encounter channels with only LOS paths and hence the Friis formula is not a very accurate description of the communication link. A two-ray model, which consists of two overlapping waves at the receiver, one direct path and one reflected wave from the ground gives a more accurate description as shown in Figure 4.2. A simple addition of a single reflected wave shows that power varies inversely with the forth power of the distance between the Tx and the Rx. This is deduced via the following treatment. From Figure 4.2, the total transmitted and received electric fields are

$$E_{TOT} = E_i + E_{LOS} \quad (4.16)$$

$$E_{TOT} = E_i + E_{LO} \quad (4.17)$$

Let E_0 is the free space electric field (in V/m) at a reference distance d_0 . Then

$$E(d, t) = \frac{E_0 d_0}{d} \cos(\omega t - \varphi) \quad (4.18)$$

where

$$\varphi = \frac{2\pi d}{\lambda} \quad (4.19)$$

and $d > d_0$. The envelop of the electric field at d meters from the transmitter at any time t is therefore

$$|E(d, t)| = \frac{E_0 d_0}{d} \quad (4.20)$$

This means the envelop is constant with respect to time.

Two propagating waves arrive at the receiver, one LOS wave which travels a distance of d^t and another ground reflected wave, that travels d^{tt} .

Mathematically,

it can be expressed as:

$$E(d^t, t) = \frac{E_0 d_0}{c} \cos(\omega t - \varphi^t) \quad (4.21)$$

where

$$\varphi^t = \omega \frac{d^t}{c} \quad (4.22)$$

and

$$E(d^{tt}, t) = \frac{E_0 d_0}{c} \cos(\omega t - \varphi^{tt}) \quad (4.23)$$

where

$$\varphi^{tt} = \omega \frac{d^{tt}}{c} \quad (4.24)$$

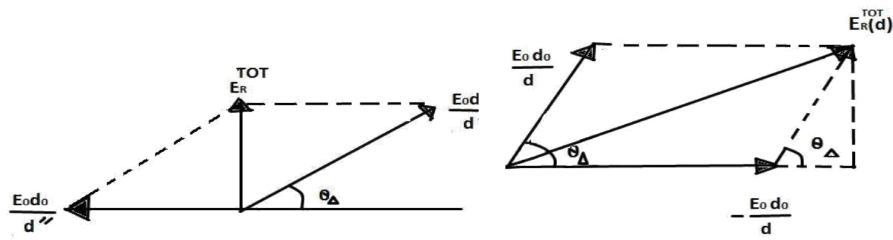


Figure 4.3: Phasor diagram of electric fields.

Figure 4.4: Equivalent phasor diagram of Figure 4.3.

According to the law of reflection in a dielectric, $\vartheta_i = \vartheta_0$ and $E_g = \Gamma E_i$ which means the total electric field,

$$E_t = E_i + E_g = E_i(1 + \Gamma). \quad (4.25)$$

For small values of ϑ_i , reflected wave is equal in magnitude and 180° out of phase with respect to incident wave. Assuming perfect horizontal electric field polarization, i.e.,

$$\Gamma_{\perp} = -1 \implies E_t = (1 - 1)E_i = 0, \quad (4.26)$$

the resultant electric field is the vector sum of E_{LOS} and E_g . This implies that,

$$E_{TOT} = |E_{LOS} + E_g|. \quad (4.27)$$

It can be therefore written that

$$E_{TOT}(d, t) = \frac{E_0 d_0}{d} \cos(\omega t - \varphi) + (-1) \frac{E_0 d_0}{d} \cos(\omega t - \varphi) \quad (4.28)$$

In such cases, the path difference is

$$\Delta = d^{tt} - d^t = \sqrt{(h_t - h_r)^2 + d^2} - \sqrt{(h_t + h_r)^2 + d^2} \quad (4.30)$$

$$(4.31)$$

$$(4.29)$$

However, when T-R separation distance is very large compared to $(ht + hr)$, then

$$\Delta \approx d$$

$$\Delta \approx d$$

Ex 3: Prove the above two equations, i.e., equation (4.29) and (4.30).

Once the path difference is known, the phase difference is

$$\vartheta_{\Delta} = \frac{2\pi\Delta}{\lambda} = \frac{\Delta\omega c}{\lambda}$$

and the time difference,

$$\tau_d = \frac{\Delta}{c} = \frac{\vartheta_{\Delta}}{2\pi f c} \quad (4.32)$$

When d is very large, then Δ becomes very small and therefore E_{LOS} and E_g are virtually identical with only phase difference, i.e.,

$$\frac{E_{OT}}{d} \approx \frac{E_{OT}}{d} e^{j\vartheta_{\Delta}} \quad (4.33)$$

Say, we want to evaluate the received E-field at any $t = t' + \frac{d}{c}$. Then,

$$E_R(d, t) = \frac{E_{OT}}{d} \cos\left(\omega_c \left(t - \frac{d}{c}\right)\right) - \frac{E_{OT}}{d} \cos\left(\omega_c \left(t - \frac{d}{c} + \vartheta_{\Delta}\right)\right) \quad (4.34)$$

$$\begin{aligned} &= \frac{E_{OT}}{d} \left[\cos\left(\omega_c \left(t - \frac{d}{c}\right)\right) - \cos\left(\omega_c \left(t - \frac{d}{c} + \vartheta_{\Delta}\right)\right) \right] \\ &= \frac{E_{OT}}{d} \left[\cos\left(\omega_c \left(t - \frac{d}{c}\right)\right) - \cos\left(\omega_c \left(t - \frac{d}{c}\right) + \vartheta_{\Delta}\right) \right] \\ &= \frac{E_{OT}}{d} \left[\cos\left(\omega_c \left(t - \frac{d}{c}\right)\right) - \cos\left(\omega_c \left(t - \frac{d}{c}\right) + \vartheta_{\Delta}\right) \right] \\ &\approx \frac{E_{OT}}{d} \left[\cos\left(\omega_c \left(t - \frac{d}{c}\right)\right) - \cos\left(\omega_c \left(t - \frac{d}{c}\right) + \vartheta_{\Delta}\right) \right] \end{aligned} \quad (4.37)$$

Using phasor diagram concept for vector addition as shown in Figures 4.3 and 4.4, we get

$$\begin{aligned} |E_R| &= \frac{E_{OT}}{d} \sqrt{\left(\frac{E_{OT}}{d} \cos(\vartheta_{\Delta})\right)^2 + \left(\frac{E_{OT}}{d} \sin(\vartheta_{\Delta})\right)^2} \\ &= \frac{E_{OT}}{d} \sqrt{(\cos(\vartheta_{\Delta}) - 1)^2 + \sin^2(\vartheta_{\Delta})} \end{aligned}$$

For $\frac{\theta}{2} < 0.5 \text{ rad}$, $\sin(\frac{\theta}{2}) \approx \frac{\theta}{2}$. Using equation (4.31) and further equation (4.38) we can then approximate that

$$\sin(\frac{\theta}{2}) \approx \frac{\pi}{\lambda} \Delta = \frac{2\pi}{\lambda d} h r < 0.5 \text{ rad.} \quad (4.39)$$

This raises the wonderful concept of 'cross-over distance' d_c , defined as

$$d > d_c = \frac{20\pi h r}{5\lambda} = \frac{4\pi h r}{\lambda}. \quad (4.40)$$

The corresponding approximate received electric field is

$$E_{TOT} \approx \frac{E_0 d}{d} \left[\frac{h}{\lambda d} + \frac{h}{d^2} \right] = k \frac{h}{d^2}. \quad (4.41)$$

(4.44)

Therefore, using equation (4.43) in (4.1), we get the received power as

$$P_r = \frac{P_t G_t G_r h^2}{L d^4} \quad (4.45)$$

The cross-over distance shows an approximation of the distance after which the received power decays with its fourth order. The basic difference between equation (4.1) and (4.45) is that when $d < d_c$, equation (4.1) is sufficient to calculate the path loss since the two-ray model does not give a good result for a short distance due to the oscillation caused by the constructive and destructive combination of the two rays, but whenever we distance crosses the 'cross-over distance', the power falls off rapidly as well as two-ray model approximation gives better result than Friis equation.

Observations on Equation (4.45): The important observations from this equation are:

1. This equation gives fair results when the T-R separation distance crosses the cross-over distance.

In that case, the power decays as the fourth power

1. of distance

$$P_r(d) = \frac{K}{d^4} \quad (4.46)$$

with K being a constant.

Path loss is independent of frequency

2. (wavelength).

Received power is also proportional to h^2 and h^2 , meaning, if height of any of

3. the

t r

antennas is increased, received power increases.

Diffraction

Diffraction is the phenomena that explain the digression of a wave from a straight line path, under the influence of an obstacle, so as to propagate behind the obstacle. It is an inherent feature of a wave be it longitudinal or transverse. For e.g the sound can be heard in a room, where the source of the sound is another room without having any line of sight. The similar phenomenon occurs for light also but the diffracted light intensity is not noticeable. This is because the obstacle or slit need to be of the order of the wavelength of the wave to have a significant effect. Thus radiation from a point source radiating in all directions can be received at any

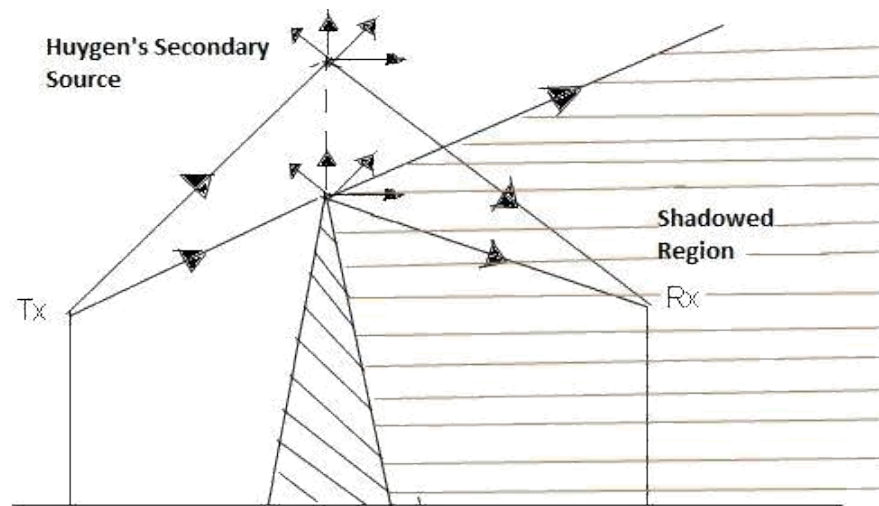


Figure 4.5: Huygen's secondary wavelets.

point, even behind an obstacle (unless it is not completely enveloped by it), as shown in Figure 4.5. Though the intensity received gets smaller as receiver is moved into the shadowed region. Diffraction is explained by Huygens-Fresnel principle which states that all points on a wavefront can be considered as the point source for secondary wavelets which form the secondary wavefront in the direction of the propagation. Normally, in absence of an obstacle, the sum of all wave sources is zero at a point not in the direct path of the wave and thus the wave travels in the straight line. But in the case of an obstacle, the effect of wave source behind the obstacle cannot be felt and the sources around the obstacle contribute to the secondary wavelets in the shadowed region, leading to bending of wave. In mobile communication, this has a great advantage since, by diffraction (and scattering, reflection), the receiver is able to receive the signal even when not in line of sight of the transmitter. This we show in the subsection given below.

Knife-Edge Diffraction Geometry

As shown in Figure 4.6, consider that there's an impenetrable obstruction of height h at a distance of d_1 from the transmitter and d_2 from the receiver. The path difference between direct path and the diffracted path is

$$\delta = \sqrt{2 + h^2} + \sqrt{d^2 + h^2} - (d_1 + d_2)$$

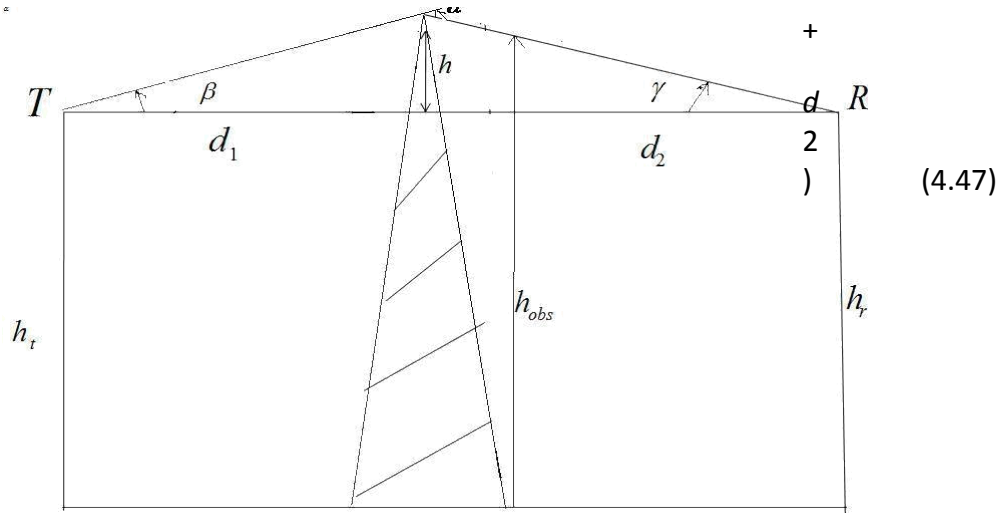


Figure 4.6: Diffraction through a sharp edge.

which can be further simplified as

$$\begin{aligned} \delta &= \frac{d_1(1 + h^2/2d_1^2)}{1} + \frac{d_2(1 + h^2/2d_2^2)}{2} - (d_1 + d_2) \\ &= h^2/(2d_1) + h^2/(2d_2) = h^2(d_1 + d_2)/(2d_1d_2). \end{aligned} \quad (4.48)$$

Thus the phase difference equals

$$\varphi = 2\pi\delta/\lambda = 2\pi h^2(d_1 + d_2)/\lambda^2(d_1d_2). \quad (4.49)$$

With the following considerations that

$$\alpha = \beta + \gamma \quad (4.50)$$

and

$$\alpha \approx \tan\alpha \quad (4.51)$$

we can write,

$$\alpha \tan\alpha = \tan\beta + \tan\gamma = h/d_1 + h/d_2 = h(d_1 + d_2)/d_1d_2. \quad (4.52)$$

In order to normalize this, we usually use a Fresnel-Kirchoff diffraction parameter v , expressed as

$$v = h \sqrt{\frac{2(d_1 + d_2)/(\lambda d_1 d_2)}{2}} = \alpha \sqrt{\frac{2d_1 d_2}{\lambda(d_1 + d_2)}} \quad (4.53)$$

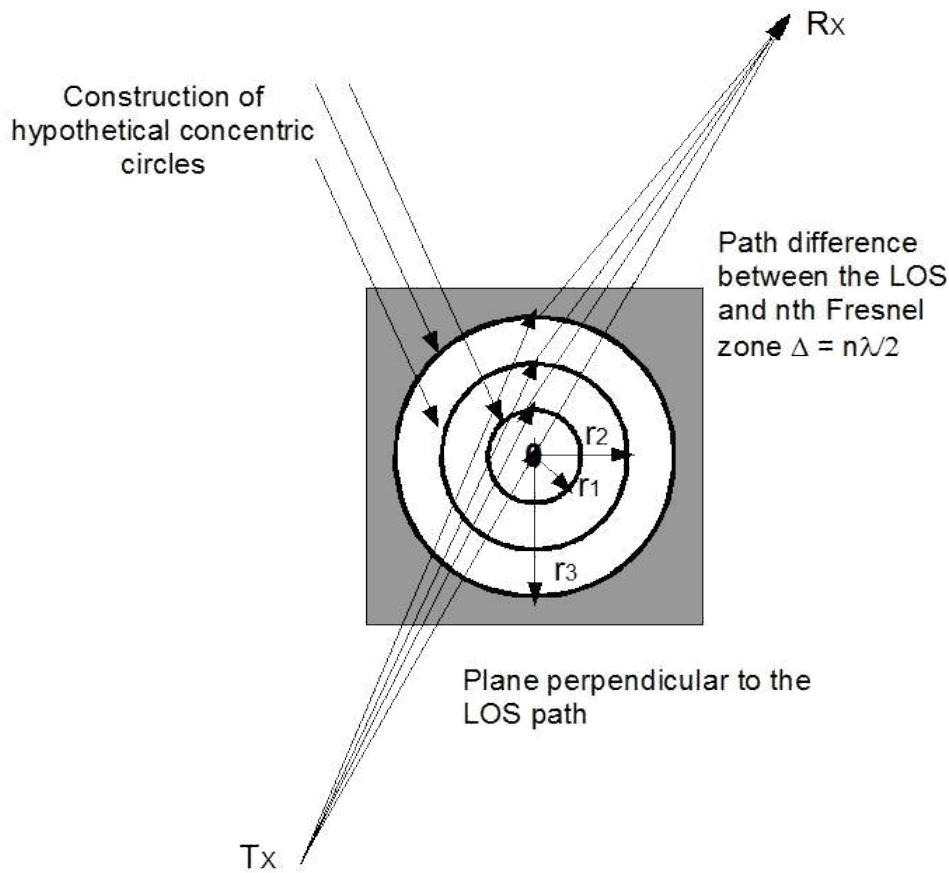


Figure 4.7: Fresnel zones.

and therefore the phase difference becomes

$$\varphi = \pi v^2/2. \quad (4.54)$$

From this, we can observe that: (i) phase difference is a function of the height of the obstruction, and also, (ii) phase difference is a function of the position of the obstruction from transmitter and receiver.

Fresnel Zones: the Concept of Diffraction Loss

As mentioned before, the more is the object in the shadowed region greater is the diffraction loss of the signal. The effect of diffraction loss is explained by Fresnel zones as a function of the path difference. The successive Fresnel zones are limited by the circular periphery through which the path difference of the secondary waves is $n\lambda/2$ greater than total length of the LOS path, as shown in

Figure 4.7. Thus successive Fresnel zones have phase difference of π which means they alternatively

provide constructive and destructive interference to the received signal. The radius of each Fresnel zone is maximum at middle of transmitter and receiver (i.e. when $d_1 = d_2$) and decreases as moved to either side. It is seen that the loci of a Fresnel zone varied over d_1 and d_2 forms an ellipsoid with the transmitter and receiver at its foci. Now, if there's no obstruction, then all Fresnel zones result in only the direct LOS propagation and no diffraction effects are observed. But if an obstruction is present, depending on its geometry, it obstructs contribution from some of the secondary wavelets, resulting in diffraction and also the loss of energy, which is the vector sum of energy from unobstructed sources. please note that height of the obstruction can be positive zero and negative also. The diffraction losses are minimum as long as obstruction doesn't block volume of the 1st Fresnel zone. As a rule of thumb, diffraction effects are negligible beyond 55% of 1st Fresnel zone.

Ex 4: Calculate the first Fresnel zone obstruction height maximum for $f = 800$ MHz.

Solution:

$$\lambda = \frac{c}{f} = \frac{3 \times 10^8}{8 \times 10^2 \times 10^6} = \frac{3}{8} \text{ m}$$

$$H = \frac{\lambda (d_1 + d_2)}{8}$$

$$H_1 = \frac{250 \times 250}{8 \times 500} = 6.89 \text{ m}$$

$$\text{Thus } H_1 = 10 + 6.89 = 16.89 \text{ m}$$

(b)

$$H_2 = \frac{0.3 \times 100 \times 400}{8 \times 500} = 10 (0.3) = 5.48 \text{ m}$$

Thus

$$H_2 = 10 + 5.6 = 15.48 \text{ m}$$

. To have good power strength, obstacle should be within the 60% of the first fresnel zone.

Ex 5: Given $f=900$ MHz, $d_1 = d_2 = 1$ km, $h = 25$ m, where symbols have usual meaning. Compute the diffraction loss. Also find out in which Fresnel zone the tip of the obstruction lies.

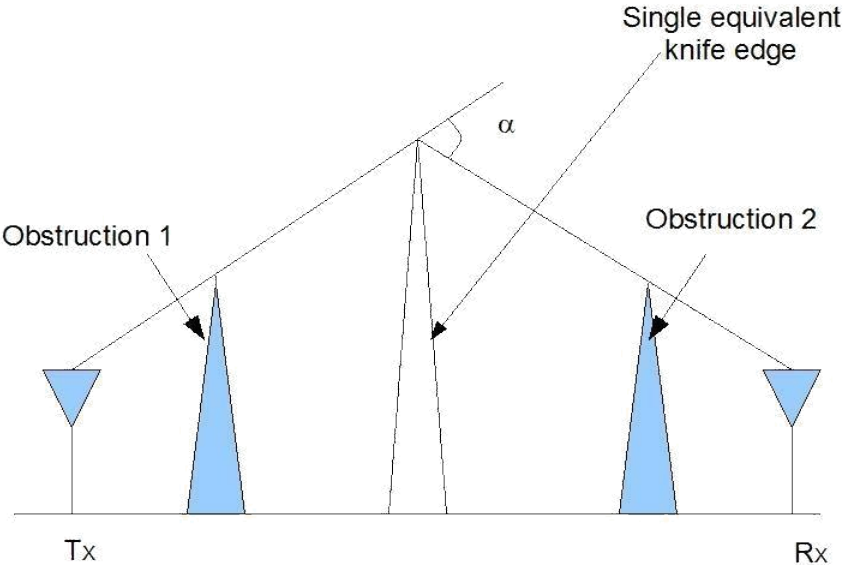


Figure 4.8: Knife-edge Diffraction Model

Given,

$$tt_d(dB) = 20 \log(0.5 - 0.62v) \quad -1 < v \leq 0$$

$$tt_d(dB) = 20 \log(0.225/v) \quad v > 2.24$$

Solution:

$$v = h \frac{2 \sqrt{d_1 + d_2}}{\lambda d_1 d_2} = 25 \frac{1}{10} = 2.74$$

$$G_d(dB) = 20 \log\left(\frac{22}{5v}\right) = -21.7 \text{ dB}$$

Since loss = $-tt_d$ (dB) = 21.7 dB

$$n = \sqrt{(2.74)^2 - 3.5} = 2$$

Thus $n=4$.

4.5.3 Knife-edge diffraction model

Knife-edge diffraction model is one of the simplest diffraction model to estimate the diffraction loss. It considers the object like hill or mountain as a knife edge sharp

object. The electric field strength, E_d of a knife-edge diffracted wave is given

by

$$E_d/E_0 = F(v) = (1 + j)/2 \int_v^{\infty} (\exp(-j\pi t^2)/2) dt. \quad (4.55)$$

The diffraction gain due to presence of knife edge can be given as

$$tt_d(db) = 20 \log |F(v)| \quad (4.56)$$

$$tt_d(db) = 0 \quad v \leq -1 \quad (4.57)$$

$$tt_d(db) = 20 \log(0.5 - 0.62) \quad -1 \leq v \leq 0 \quad (4.58)$$

$$tt_d(db) = 20 \log(0.5 \exp(-0.95v)) \quad 0 \leq v \leq 1 \quad (4.59)$$

$$tt_d(db) = 20 \log(0.4 - \sqrt{0.1184 - (0.38 - 0.1v^2)}) \quad 1 \leq v \leq 2.4 \quad (4.60)$$

$$tt_d(db) = 20 \log(0.225/v) \quad v > 2.4 \quad (4.61)$$

When there are more than one obstruction, then the equivalent model can be found by one knife-edge diffraction model as shown in Figure 4.8.

Scattering

The actual received power at the receiver is somewhat stronger than claimed by the models of reflection and diffraction. The cause is that the trees, buildings and lamp-posts scatter energy in all directions. This provides extra energy at the receiver. Roughness is tested by a Rayleigh criterion, which defines a critical height hc of

surface protuberances for a given angle of incidence ϑ ,
given by,

$$hc = \frac{\lambda}{8 \sin \vartheta} \quad (4.10)$$

A surface is smooth if its minimum to maximum protuberance h is less than hc , and rough if protuberance is greater than hc . In case of rough surfaces, the surface reflection coefficient needs to be multiplied by a scattering loss factor ρ_S , given by

$$\frac{\pi \sigma_h \sin \vartheta}{2} \quad (4.11)$$

$$\rho S = \exp\left(-8 \frac{\sigma_h^2}{\lambda^2} \sin^2 \theta\right)$$

where σ_h is the standard deviation of the Gaussian random variable h . The following result is a better approximation to the observed value

$$\rho S = \exp\left(-8 \frac{\pi \sigma_h \sin \theta}{\lambda}\right) \left[\exp\left(-8 \frac{\pi \sigma_h \sin \theta}{\lambda}\right) \right] \quad (4.12)$$

Outdoor Propagation Models

There are many empirical outdoor propagation models such as Longley-Rice model, Durkin's model, Okumura model, Hata model etc. Longley-Rice model is the most commonly used model within a frequency band of 40 MHz to 100 GHz over different terrains. Certain modifications over the rudimentary model like an extra urban factor (UF) due to urban clutter near the receiver is also included in this model. Below, we discuss some of the outdoor models, followed by a few indoor models too.

3.10.1 Longley-Rice Model

The Longley-Rice model [Ric67], [Lon68] is applicable to point-to-point communication systems in the frequency range from 40 MHz to 100 GHz, over different kinds of terrain. The median transmission loss is predicted using the path geometry of the terrain profile and the refractivity of the troposphere. Geometric optics techniques (primarily the 2-ray ground reflection model) are used to predict signal strengths within the radio horizon. Diffraction losses over isolated obstacles are estimated using the Fresnel-Kirchoff knife-edge models. Forward scatter theory is used to make troposcatter predictions over long distances, and far field diffraction losses in double horizon paths are predicted using a modified Van der Pol-Bremmer method. The Longley-Rice propagation prediction model is also referred to as the *ITS irregular terrain model*.

The Longley-Rice model is also available as a computer program [Lon78] to calculate large-scale median transmission loss relative to free space loss over irregular terrain for frequencies between 20 MHz and 10 GHz. For a given transmission path, the program takes as its input the transmission frequency, path length, polarization, antenna heights, surface refractivity, effective radius of earth, ground conductivity, ground dielectric constant, and climate. The program also operates on path-specific parameters such as horizon distance of the anten-

nas, horizon elevation angle, angular trans-horizon distance, terrain irregularity and other specific inputs.

The Longley-Rice method operates in two modes. When a detailed terrain path profile is available, the path-specific parameters can be easily determined and the prediction is called a *point-to-point mode* prediction. On the other hand, if the terrain path profile is not available, the Longley-Rice method provides techniques to estimate the path-specific parameters, and such a prediction is called an *area mode* prediction.

There have been many modifications and corrections to the Longley-Rice model since its original publication. One important modification [Lon78] deals with radio propagation in urban areas, and this is particularly relevant to mobile radio. This modification introduces an excess term as an allowance for the additional attenuation due to urban clutter near the receiving antenna. This extra term, called the *urban factor (UF)*, has been derived by comparing the predictions by the original Longley-Rice model with those obtained by Okumura [Oku68].

One shortcoming of the Longley-Rice model is that it does not provide a way of determining corrections due to environmental factors in the immediate vicinity of the mobile receiver, or consider correction factors to account for the effects of buildings and foliage. Further, multipath is not considered.

Okumura Model

The Okumura model is used for Urban Areas is a Radio propagation model that is used for signal prediction. The frequency coverage of this model is in the range of 200 MHz to 1900 MHz and distances of 1 Km to 100 Km. It can be applicable for base station effective antenna heights (ht) ranging from 30 m to 1000 m.

Okumura used extensive measurements of base station-to-mobile signal attenuation throughout Tokyo to develop a set of curves giving median attenuation relative to free space (Amu) of signal propagation in irregular terrain. The empirical path-loss formula of Okumura at distance d parameterized by the carrier frequency fc is given by

$$PL(d)dB = L(fc, d) + Amu(fc, d) - tt(ht) - tt(hr) - ttAREA \quad (4.67)$$

where $L(fc, d)$ is free space path loss at distance d and carrier frequency fc , $Amu(fc, d)$

is the median attenuation in addition to free-space path loss across all environments, $tt(ht)$ is the base station antenna height gain factor, $tt(hr)$ is the mobile antenna height gain factor, $ttAREA$ is the gain due to type of environment. The values of $Amu(fc, d)$ and $ttAREA$ are obtained from Okumura's empirical plots. Okumura derived empirical formulas for $tt(ht)$ and $tt(hr)$ as follows:

$$tt(ht) = 20 \log_{10}(ht/200), \quad 30m < ht < 1000m \quad (4.68)$$

$$tt(hr) = 10 \log_{10}(hr / 3), \quad hr \leq 3m \quad (4.69)$$

$$tt(hr) = 20 \log_{10}(hr / 3), \quad 3m < hr < 10m \quad (4.70)$$

Correlation factors related to terrain are also developed in order to improve the models accuracy. Okumura's model has a 10-14 dB empirical standard deviation between the path loss predicted by the model and the path loss associated with one of the measurements used to develop the model.

Hata Model

The Hata model is an empirical formulation of the graphical path-loss data provided by the Okumura and is valid over roughly the same range of frequencies, 150-1500 MHz. This empirical formula simplifies the calculation of path loss because it is closed form formula and it is not based on empirical curves for the different parameters. The standard formula for empirical path loss in urban areas under the Hata model is

$$P_{L,urban}(d)dB = 69.55 + 26.16 \log_{10}(fc) - 13.82 \log_{10}(ht) - a(hr) + (44.9 - 6.55 \log_{10}(ht)) \log_{10}(d)$$

The parameters in this model are same as in the Okumura model, and $a(hr)$ is a correction factor for the mobile antenna height based on the size of coverage area. For small to medium sized cities this factor is given by

$$a(hr) = (1.11 \log_{10}(fc) - 0.7)hr - (1.56 \log_{10}(fc) - 0.8)dB$$

and for larger cities at a frequencies $fc > 300$ MHz by

$$a(hr) = 3.2(\log_{10}(11.75hr))^2 - 4.97dB$$

else it is

$$a(hr) = 8.29(\log_{10}(1.54hr))^2 - 1.1dB$$

Corrections to the urban model are made for the suburban, and is given by

$$PL, \text{suburban}(d)dB = PL, \text{urban}(d)dB - 2(\log_{10}(fc/28))^2 - 5.4 \quad (4.72)$$

Unlike the Okumura model, the Hata model does not provide for any specific path-correlation factors. The Hata model well approximates the Okumura model for distances $d > 1$ Km. Hence it is a good model for first generation cellular systems, but it does not model propagation well in current cellular systems with smaller cell sizes and higher frequencies. Indoor environments are also not captured by the Hata model.

3.10.5 PCS Extension to Hata Model

The European Co-operative for Scientific and Technical research (EURO-COST) formed the COST-231 working committee to develop an extended version of the Hata model. COST-231 proposed the following formula to extend Hata's model to 2 GHz. The proposed model for path loss is [EUR91]

$$L_{50}(urban) = 46.3 + 33.9 \log f_c - 13.82 \log h_{te} - a(h_{re}) + (44.9 - 6.55 \log h_{te}) \log d + C_M \quad (3.87)$$

where $a(h_{re})$ is defined in equations (3.83), (3.84.a), and (3.84.b) and

$$C_M = \begin{cases} 0 \text{ dB} & \text{for medium sized city and suburban areas} \\ 3 \text{ dB} & \text{for metropolitan centers} \end{cases} \quad (3.88)$$

The COST-231 extension of the Hata model is restricted to the following range of parameters:

$$\begin{aligned} f &: 1500 \text{ MHz to } 2000 \text{ MHz} \\ h_{te} &: 30 \text{ m to } 200 \text{ m} \\ h_{re} &: 1 \text{ m to } 10 \text{ m} \\ d &: 1 \text{ km to } 20 \text{ km} \end{aligned}$$

3.10.6 Walfisch and Bertoni Model

A model developed by Walfisch and Bertoni [Wal88] considers the impact of rooftops and building height by using diffraction to predict average signal strength at street level. The model considers the path loss, S , to be a product of three factors.

$$S = P_0 Q^2 P_1 \quad (3.89)$$

where P_0 represents free space path loss between isotropic antennas given by

$$P_0 = \left(\frac{\lambda}{4\pi R} \right)^2 \quad (3.90)$$

The factor Q^2 gives the reduction in the rooftop signal due to the row of buildings which immediately shadow the receiver at street level. The P_1 term is

based upon diffraction and determines the signal loss from the rooftop to the street.

In dB, the path loss is given by

$$S(\text{dB}) = L_0 + L_{rts} + L_{ms} \quad (3.91)$$

where L_0 represents free space loss, L_{rts} represents the “rooftop-to-street diffraction and scatter loss”, and L_{ms} denotes multiscreen diffraction loss due to the rows of buildings [Xia92]. Figure 3.25 illustrates the geometry used in the Walfisch Bertoni model [Wal88], [Mac93]. This model is being considered for use by ITU-R in the IMT-2000 standards activities.

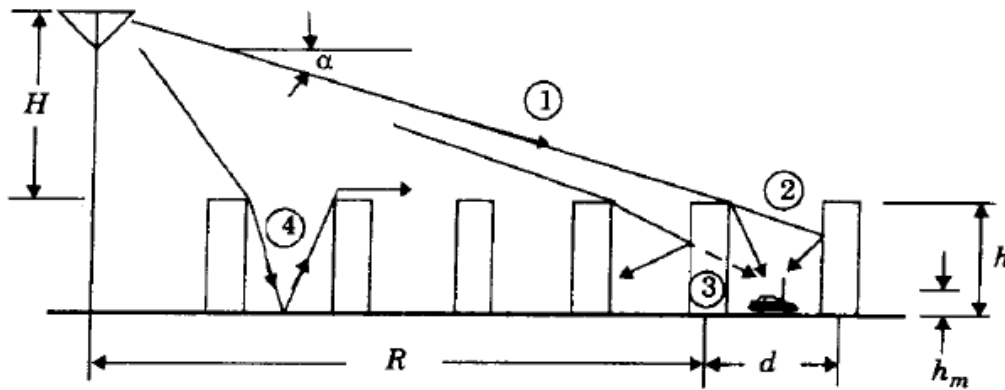


Figure 3.25

Propagation geometry for model proposed by Walfisch and Bertoni [From [Wal88] © IEEE].

3.10.7 Wideband PCS Microcell Model

Work by Feuerstein, et.al. in 1991 used a 20 MHz pulsed transmitter at 1900 MHz to measure path loss, outage, and delay spread in typical microcellular systems in San Francisco and Oakland. Using base station antenna heights of 3.7 m, 8.5 m, and 13.3 m, and a mobile receiver with an antenna height of 1.7 m above ground, statistics for path loss, multipath, and coverage area were developed from extensive measurements in line-of-sight (LOS) and obstructed (OBS) environments [Feu94]. This work revealed that a 2-ray ground reflection model (shown in Figure 3.7) is a good estimate for path loss in LOS microcells, and a simple log-distance path loss model holds well for OBS microcell environments.

For a flat earth ground reflection model, the distance d_f at which the first Fresnel zone just becomes obstructed by the ground (first Fresnel zone clearance) is given by

$$d_f = \frac{1}{\lambda} \sqrt{(\Sigma^2 - \Delta^2)^2 - 2(\Sigma^2 + \Delta^2) \left(\frac{\lambda}{2}\right)^2 + \left(\frac{\lambda}{2}\right)^4} \quad (3.92.a)$$

$$= \frac{1}{\lambda} \sqrt{16h_t^2 h_r^2 - \lambda^2 (h_t^2 + h_r^2) + \frac{\lambda^4}{16}}$$

For LOS cases, a double regression path loss model that uses a regression breakpoint at the first Fresnel zone clearance was shown to fit well to measurements. The model assumes omnidirectional vertical antennas and predicts average path loss as

$$PL(d) = \begin{cases} 10n_1 \log(d) + p_1 & \text{for } 1 < d < d_f \\ 10n_2 \log(d/d_f) + 10n_1 \log d_f + p_1 & \text{for } d > d_f \end{cases} \quad (3.92.b)$$

where p_1 is equal to $PL(d_0)$ (the path loss in decibels at the reference distance of $d_0 = 1$ m), d is in meters and n_1, n_2 are path loss exponents which are a function of transmitter height, as given in Figure 3.26. It can easily be shown that at 1900 MHz, $p_1 = 38.0$ dB.

For the OBS case, the path loss was found to fit the standard log-distance path loss law of equation (3.69.a)

$$PL(d) [dB] = 10n \log(d) + p_1 \quad (3.92.c)$$

where n is the OBS path loss exponent given in Figure 3.26 as a function of transmitter height. The standard deviation (in dB) of the log-normal shadowing component about the distance-dependent mean was found from measurements using the techniques described in Chapter 3, section 3.10.2. The log-normal shadowing component is also listed as a function of height for both the LOS and OBS microcell environments. Figure 3.26 indicates that the log-normal shadowing component is between 7 and 9 dB regardless of antenna height. It can be seen that LOS environments provide slightly less path loss than the theoretical 2-ray ground reflected model, which would predict $n_1 = 2$ and $n_2 = 4$.

Transmitter Antenna Height	1900 MHz LOS			1900 MHz OBS	
	n_1	n_2	σ (dB)	n	σ (dB)
Low (3.7m)	2.18	3.29	8.76	2.58	9.31
Medium (8.5m)	2.17	3.36	7.88	2.56	7.67
High (13.3m)	2.07	4.16	8.77	2.69	7.94

Figure 3.26

Indoor Propagation Models

The indoor radio channel differs from the traditional mobile radio channel in ways - the distances covered are much smaller, and the variability of the environment is much greater for smaller range of Tx-Rx separation distances. Features such as lay-out of the building, the construction materials, and the building type strongly influence the propagation within the building. Indoor radio propagation is dominated by the same mechanisms as outdoor: reflection, diffraction and

scattering with variable conditions. In general, indoor channels may be classified as either line-of-sight or obstructed.

Partition Losses Inside a Floor (Intra-floor)

The internal and external structure of a building formed by partitions and obstacles vary widely. Partitions that are formed as a part of building structure are called hard partitions, and partitions that may be moved and which do not span to the ceiling are called soft partitions. Partitions vary widely in their physical and electrical characteristics, making it difficult to apply general models to specific indoor installations.

Partition Losses Between Floors (Inter-floor)

The losses between floors of a building are determined by the external dimensions and materials of the building, as well as the type of construction used to create the floors and the external surroundings. Even the number of windows in a building and the presence of tinting can impact the loss between floors.

Log-distance Path Loss Model

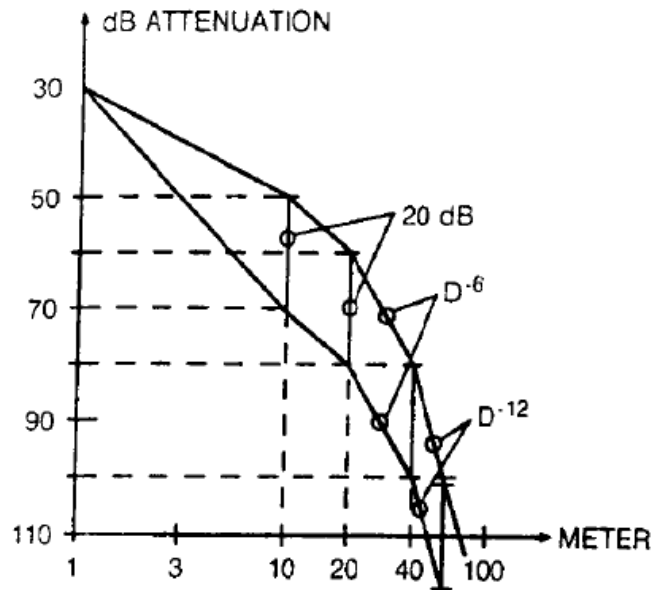
It has been observed that indoor path loss obeys the distance power law given by

$$PL(dB) = PL(d_0) + 10n \log_{10}(d/d_0) + X\sigma \quad (4.73)$$

where n depends on the building and surrounding type, and $X\sigma$ represents a normal random variable in dB having standard deviation of σ dB.

3.11.4 Ericsson Multiple Breakpoint Model

The Ericsson radio system model was obtained by measurements in a multiple floor office building [Ake88]. The model has four breakpoints and considers both an upper and lower bound on the path loss. The model also assumes that there is 30 dB attenuation at $d_0 = 1$ m, which can be shown to be accurate for $f = 900$ MHz and unity gain antennas. Rather than assuming a log-normal shadowing component, the Ericsson model provides a deterministic limit on the range of path loss at a particular distance. Bernhardt [Ber89] used a uniform distribution to generate path loss values within the maximum and minimum range as a function of distance for in-building simulation. Figure 3.27 shows a plot of in-building path loss based on the Ericsson model as a function of distance.



3.11.5 Attenuation Factor Model

An in-building propagation model that includes the effect of building type as well as the variations caused by obstacles was described by Seidel [Sei92b]. This model provides flexibility and was shown to reduce the standard deviation between measured and predicted path loss to around 4 dB, as compared to 13 dB when only a log-distance model was used in two different buildings. The attenuation factor model is given by

buildings or with outdoor systems. As with propagation measurements between floors, it is difficult to determine exact models for penetration as only a limited number of experiments have been published, and they are sometimes difficult to compare. However, some generalizations can be made from the literature. In measurements reported to date, signal strength received inside a building increases with height. At the lower floors of a building, the urban clutter induces greater attenuation and reduces the level of penetration. At higher floors, a LOS path may exist, thus causing a stronger incident signal at the exterior wall of the building.

$$\overline{PL}(d)[\text{dB}] = \overline{PL}(d_0)[\text{dB}] + 10n_{SF}\log\left(\frac{d}{d_0}\right) + FAF[\text{dB}] \quad (3.94)$$

where n_{SF} represents the exponent value for the “same floor” measurement. Thus, if a good estimate for n exists (e.g., selected from Table 3.4 or Table 3.6) on the same floor, then the path loss on a different floor can be predicted by adding an appropriate value of FAF (e.g., selected from Table 3.5). Alternatively, in equation (3.94), FAF may be replaced by an exponent which already considers the effects of multiple floor separation.

$$\overline{PL}(d)[\text{dB}] = \overline{PL}(d_0) + 10n_{MF}\log\left(\frac{d}{d_0}\right) \quad (3.95)$$

where n_{MF} denotes a path loss exponent based on measurements through multiple floors.

Table 3.7 illustrates typical values of n for a wide range of locations in many buildings. This table also illustrates how the standard deviation decreases as the average region becomes smaller and more site specific. Scatter plots illustrating actual measured path loss in two multi-floored office buildings are shown in Figure 3.28 and Figure 3.29.

RF penetration has been found to be a function of frequency as well as height within the building. The antenna pattern in the elevation plane also plays an important role in how much signal penetrates a building from the outside. Most measurements have considered outdoor transmitters with antenna heights far less than the maximum height of the building under test. Measurements in Liverpool [Tur87] showed that penetration loss decreases with increasing frequency. Specifically, penetration attenuation values of 16.4 dB, 11.6 dB, and 7.6 dB were measured on the ground floor of a building at frequencies of 441 MHz, 896.5 MHz, and 1400 MHz, respectively. Measurements by Turkmani [Tur92] showed penetration loss of 14.2 dB, 13.4 dB, and 12.8 dB for 900 MHz, 1800 MHz, and 2300 MHz, respectively. Measurements made in front of windows indicated 6 dB less penetration loss on average than did measurements made in parts of the buildings without windows.

3.13 Ray Tracing and Site Specific Modeling

In recent years, the computational and visualization capabilities of computers have accelerated rapidly. New methods for predicting radio signal coverage involve the use of Site Specific (SISP) propagation models and *graphical infor-*

mation system (GIS) databases [Rus93]. SISP models support ray tracing as a means of deterministically modeling any indoor or outdoor propagation environment. Through the use of building databases, which may be drawn or digitized using standard graphical software packages, wireless system designers are able to include accurate representations of building and terrain features.

For outdoor propagation prediction, ray tracing techniques are used in conjunction with aerial photographs so that three-dimensional (3-D) representations of buildings may be integrated with software that carries out reflection, diffraction, and scattering models. Photogrammetric techniques are used to convert aerial or satellite photographs of cities into usable 3-D databases for the models [Sch92], [Ros93], [Wag94]. In indoor environments, architectural drawings provide a site specific representation for propagation models [Val93], [Sei94], [Kre94].

As building databases become prevalent, wireless systems will be developed using computer aided design tools that provide deterministic, rather than statistical, prediction models for large-scale path loss in a wide range of operating environments.

Walker [Wal92] measured radio signals into fourteen different buildings in Chicago from seven external cellular transmitters. Results showed that building penetration loss decreased at a rate of 1.9 dB per floor from the ground level up to the fifteenth floor and then began increasing above the fifteenth floor. The increase in penetration loss at higher floors was attributed to shadowing effects of adjacent buildings. Similarly, Turkmani [Tur87] reported penetration loss decreased at a rate of 2 dB per floor from the ground level up to the ninth floor and then increased above the ninth floor. Similar results were also reported by Durante [Dur73].

Measurements have shown that the percentage of windows, when compared with the building face surface area, impacts the level of RF penetration loss, as does the presence of tinted metal in the windows. Metallic tints can provide from 3 dB to 30 dB RF attenuation in a single pane of glass. The angle of incidence of the transmitted wave upon the face of the building also has a strong impact on the penetration loss, as was shown by Horikishi [Hor86].

Unit-3 Mobile Radio Propagation:

Small- Scale Fading and Multipath

Multipath Propagation

In wireless telecommunications, multipath is the propagation phenomenon that results in radio signals reaching the receiving antenna by two or more paths. Causes of multipath include atmospheric ducting, ionospheric reflection and refraction, and reflection from water bodies and terrestrial objects such as mountains and buildings. The effects of multipath include constructive and destructive interference, and phase shifting of the signal. In digital radio communications (such as GSM) multipath can cause errors and affect the quality of communications. We discuss all the related issues in this chapter.

Multipath & Small-Scale Fading

Multipath signals are received in a terrestrial environment, i.e., where different forms of propagation are present and the signals arrive at the receiver from transmitter via a variety of paths. Therefore there would be multipath interference, causing multi-path fading. Adding the effect of movement of either Tx or Rx or the surrounding clutter to it, the received overall signal amplitude or phase changes over a small amount of time. Mainly this causes the fading.

Fading

The term **fading**, or, small-scale fading, means rapid fluctuations of the amplitudes, phases, or multipath delays of a radio signal over a short period or short travel distance. This might be so severe that large scale radio propagation loss effects might be ignored.

Multipath Fading Effects

In principle, the following are the main multipath effects:

1. Rapid changes in signal strength over a small travel distance or time interval.
2. Random frequency modulation due to varying Doppler shifts on different multipath signals.
3. Time dispersion or echoes caused by multipath propagation delays.

Factors Influencing Fading

The following physical factors influence small-scale fading in the radio propagation channel:

- (1) Multipath propagation** – Multipath is the propagation phenomenon that results in radio signals reaching the receiving antenna by two or more paths. The effects of multipath include constructive and destructive interference, and phase shifting of the signal.
- (2) Speed of the mobile** – The relative motion between the base station and the mobile results in random frequency modulation due to different Doppler shifts on each of the multipath components.
- (3) Speed of surrounding objects** – If objects in the radio channel are in motion, they induce a time varying Doppler shift on multipath components. If the surrounding objects move at a greater rate than the mobile, then this effect dominates fading.
- (4) Transmission Bandwidth of the signal** – If the transmitted radio signal bandwidth is greater than the “bandwidth” of the multipath channel (quantified by coherence bandwidth), the received signal will be distorted.

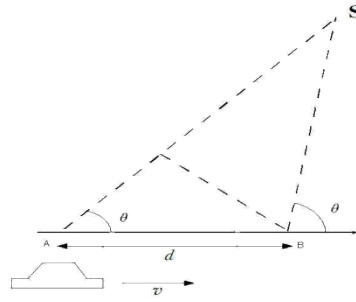


Figure 5.1: Illustration of Doppler effect.

Doppler Shift

The Doppler effect (or Doppler shift) is the change in frequency of a wave for an observer moving relative to the source of the wave. In classical physics (waves in a medium), the relationship between the observed frequency f and the emitted frequency f_0 is given by:

$$f = \frac{v \pm v_r}{v \pm v_s} f_0 \quad (5.10)$$

where v is the velocity of waves in the medium, v_s is the velocity of the source relative to the medium and v_r is the velocity of the receiver relative to the medium.

In mobile communication, the above equation can be slightly changed according to our convenience since the source (BS) is fixed and located at a remote elevated level from ground. The expected Doppler shift of the EM wave then comes out to be $\pm \frac{v_r}{c} f_0$ or, $\pm \frac{v_r}{\lambda}$. As the BS is located at an elevated place, a $\cos \phi$ factor would also be multiplied with this. The exact scenario, as given in Figure 5.1, is illustrated below.

Consider a mobile moving at a constant velocity v , along a path segment length d between points A and B, while it receives signals from a remote BS source S. The difference in path lengths traveled by the wave from source S to the mobile at points A and B is $\Delta l = d \cos \theta = v \Delta t \cos \theta$, where Δt is the time required for the mobile to travel from A to B, and θ is assumed to be the same at points A and B since the source is assumed to be very far away. The phase change in the received signal due to the difference in path lengths is therefore

$$\Delta \phi = \frac{2\pi \Delta l}{\lambda} = \frac{2\pi v \Delta t}{\lambda} \cos \theta \quad (5.11)$$

and hence the apparent change in frequency, or Doppler shift (f_d) is

$$f_d = \frac{1}{\Delta t} \frac{\Delta \phi}{2\pi} = \frac{v}{\lambda} \cos \theta \quad (5.12)$$

Example 1

An aircraft is heading towards a control tower with 500 kmph, at an elevation of 20° . Communication between aircraft and control tower occurs at 900 MHz. Find out the expected Doppler shift.

Solution As given here,

$$v = 500 \text{ kmph}$$

the horizontal component of the velocity is

$$v^t = v \cos \theta = 500 \times \cos 20^\circ = 130 \text{ m/s}$$

Hence, it can be written that

$$\lambda = \frac{900 \times 10^6}{3 \times 10^8} = 3 \text{ m}$$
$$f_d = \frac{130}{3} = 390 \text{ Hz}$$

If the plane banks suddenly and heads for other direction, the Doppler shift change will be 390 Hz to -390 Hz.

Impulse Response Model of a Multipath Channel

Mobile radio channel may be modeled as a linear filter with time varying impulse response in continuous time. To show this, consider time variation due to receiver motion and time varying impulse response $h(d, t)$ and $x(t)$, the transmitted signal. The received signal $y(d, t)$ at any position d would be

$$y(d, t) = x(t) * h(d, t) = \int_{-\infty}^{\infty} x(\tau) h(d, t - \tau) d\tau \quad (5.13)$$

For a causal system: $h(d, t) = 0$, for $t < 0$ and for a stable system $\int_{-\infty}^{\infty} |h(d, t)| dt < \infty$

∞

Applying causality condition in the above equation, $h(d, t - \tau) = 0$ for $t - \tau < 0 \Rightarrow \tau > t$, i.e., the integral limits are changed to

$$y(d, t) = \int_{-\infty}^t x(\tau) h(d, t - \tau) d\tau.$$

Since the receiver moves along the ground at a constant velocity v , the position of the receiver is $d = vt$, i.e.,

$$y(vt, t) = \int_{-\infty}^t x(\tau) h(vt, t - \tau) d\tau.$$

Since v is a constant, $y(vt, t)$ is just a function of t . Therefore the above equation can be expressed as

$$y(t) = \int_{-\infty}^t x(\tau) h(vt, t - \tau) d\tau = x(t) * h(vt, t) = x(t) * h(d, t) \quad (5.14)$$

It is useful to discretize the multipath delay axis τ of the impulse response into equal time delay segments called **excess delay bins**, each bin having a time delay width

equal to $(\tau_{i+1} - \tau_i) = \Delta\tau$ and $\tau_i = i\Delta\tau$ for $i \in \{0, 1, 2, \dots, N-1\}$, where N represents the total number of possible equally-spaced multipath components, including the first arriving component. The useful frequency span of the model is $\frac{2}{\Delta\tau}$. The model may be used to analyze transmitted RF signals having bandwidth less than

$\frac{2}{\Delta\tau}$.

If there are N multipaths, maximum excess delay is given by $N \Delta\tau$.

$$\{y(t) = x(t) * h(t, \tau_i) | i = 0, 1, \dots, N-1\} \quad (5.15)$$

Bandpass channel impulse response model is

$$x(t) \rightarrow h(t, \tau) = \text{Re}\{h_b(t, \tau) e^{j\omega_c t}\} \rightarrow y(t) = \text{Re}\{r(t) e^{j\omega_c t}\} \quad (5.16)$$

Baseband equivalent channel impulse response model is given by

$$c(t) \rightarrow \frac{1}{2} h_b(t, \tau) \rightarrow r(t) = c(t) * \frac{1}{2} h_b(t, \tau) \quad (5.17)$$

Average power is

$$\overline{x^2(t)} = \frac{1}{2} \overline{|c(t)|^2} \quad (5.18)$$

The baseband impulse response of a multipath channel can be expressed as

$$h_b(t, \tau) = \sum_{i=0}^{N-1} a_i(t, \tau) \exp[j(2\pi f_c \tau_i(t) + \phi_i(t, \tau))] \delta(\tau - \tau_i(t)) \quad (5.19)$$

$$i=0$$

where $a_i(t, \tau)$ and $\tau_i(t)$ are the real amplitudes and excess delays, respectively, of the i th multipath component at time t . The phase term $2\pi f_c \tau_i(t) + \phi_i(t, \tau)$ in the above equation represents the phase shift due to free space propagation of the i th multipath component, plus any additional phase shifts which are encountered in the channel.

If the channel impulse response is wide sense stationary over a small-scale time or distance interval, then

$$h_b(\tau) = \sum_{i=0}^{N-1} a_i \exp[j\theta_i] \delta(\tau - \tau_i) \quad (5.20)$$

For measuring $h_b(\tau)$, we use a probing pulse to approximate $\delta(t)$ i.e.,

$$p(t) \approx \delta(t - \tau) \quad (5.21)$$

Power delay profile is taken by spatial average of $|h_b(t, \tau)|^2$ over a local area. The received power delay profile in a local area is given by

$$p(\tau) \approx \overline{|h_b(t, \tau)|^2} \quad (5.22)$$

Relation Between Bandwidth and Received Power

In actual wireless communications, impulse response of a multipath channel is measured using channel sounding techniques. Let us consider two extreme channel sounding cases.

Consider a pulsed, transmitted RF signal

$$x(t) = \text{Re}\{p(t)e^{j2\pi f_c t}\} \quad (5.23)$$

where $p(t) = \frac{A \tau_{\max}}{T_{bb}}$ for $0 \leq t \leq T_{bb}$ and 0 elsewhere. The low pass channel output

is

$$\begin{aligned} r(t) &= \sum_{i=0}^{N-1} a_i \exp[j\theta_i] p(t - \tau_i) \\ &= \sum_{i=0}^{N-1} a_i \exp[j\theta_i] \frac{A \tau_{\max}}{T_{bb}} \text{rect}\left(t - \frac{T_b}{2} - \tau_i\right). \end{aligned}$$

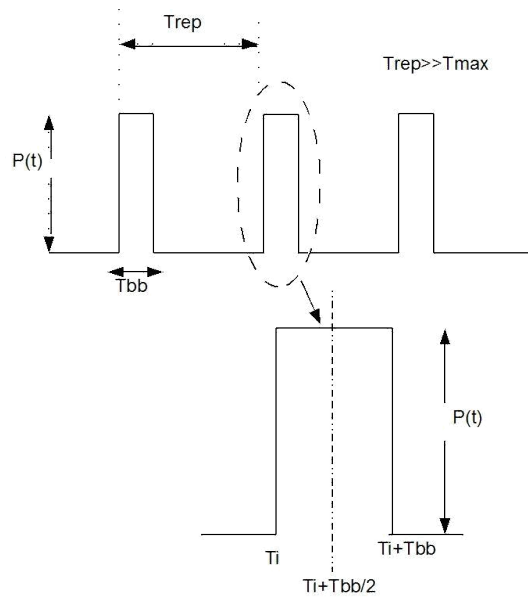


Figure 5.2: A generic transmitted pulsed RF signal.

The received power at any time t_0 is

$$\begin{aligned}
 |r(t_0)|^2 &= \frac{1}{\tau_{\max}} \int_0^{\tau_{\max}} r(t) r^*(t) dt \\
 &= \frac{1}{\tau_{\max}} \sum_{k=0}^{N-1} \frac{1}{4} a_k^2(t_0) p^2(t - \tau_k) dt \\
 &= \frac{1}{\tau_{\max}} \sum_{k=0}^{N-1} a_k^2(t_0) \int_0^{\tau_{\max}} \frac{\tau}{T_{bb}} \text{rect}(t - \tau_k) dt \\
 &= \sum_{k=0}^{N-1} a_k^2(t_0)
 \end{aligned}$$

Interpretation: If the transmitted signal is able to resolve the multipaths, then average small-scale receiver power is simply sum of average powers received from each multipath components.

$$E_{a,\theta} [P_{WB}] = E_{a,\theta} \left[\sum_{i=0}^{N-1} |a_i \exp(j\theta_i)|^2 \right] \approx \sum_{i=0}^{N-1} \frac{2}{a_i} \quad (5.24)$$

Now instead of a pulse, consider a CW signal, transmitted into the same channel and for simplicity, let the envelope be $c(t) = 2$. Then

$$r(t) = \sum_{i=0}^{N-1} a_i \exp[j\theta_i(t, \tau)] \quad (5.25)$$

and the instantaneous power is

$$|r(t)|^2 = \left| \sum_{i=0}^{N-1} a_i \exp[j\theta_i(t, \tau)] \right|^2 \quad (5.26)$$

Over local areas, a_i varies little but θ_i varies greatly resulting in large fluctuations.

$$\begin{aligned} E_{a,\theta} [P_{CW}] &= E_{a,\theta} \left[\sum_{i=0}^{N-1} |a_i \exp(j\theta_i)|^2 \right] \\ &\approx \sum_{i=0}^{N-1} a_i^2 + 2 \sum_{i=0}^{N-1} \sum_{j=i+1}^{N-1} r_{ij} \cos(\theta_i - \theta_j) \end{aligned}$$

where $r_{ij} = E_a[a_i a_j]$.

If, $r_{ij} = \cos(\theta_i - \theta_j) = 0$, then $E_{a,\theta} [P_{CW}] = E_{a,\theta} [P_{WB}]$. This occurs if multipath components are uncorrelated or if multipath phases are i.i.d over $[0, 2\pi]$.

Bottomline:

1. If the signal bandwidth is greater than multipath channel bandwidth then fading effects are negligible
2. If the signal bandwidth is less than the multipath channel bandwidth, large fading occurs due to phase shift of unresolved paths.

Linear Time Varying Channels (LTV)

The time variant transfer function(TF) of an LTV channel is FT of $h(t, \tau)$ w.r.t. τ .

$$H(f, t) = FT [h(\tau, t)] = \int_{-\infty}^{\infty} h(\tau, t) e^{-j2\pi f \tau} d\tau \quad (5.27)$$

$$h(\tau, t) = FT^{-1} [H(f, t)] = \int_{-\infty}^{\infty} H(f, t) e^{j2\pi f \tau} df \quad (5.28)$$

The received signal

$$r(t) = \int_{-\infty}^{\infty} R(f, t) e^{j2\pi f t} df \quad (5.29)$$

where $R(f, t) = H(f, t)X(f)$.

For flat fading channel, $h(\tau, t) = Z(t)\delta(\tau - \tau_i)$ where $Z(t) = \sum a_n(t)e^{-j2\pi f \tau_i n(t)}$. In this case, the received signal is

$$r(t) = \int_{-\infty}^{\infty} h(\tau, t)x(t - \tau) d\tau = Z(t)x(t - \tau_i) \quad (5.30)$$

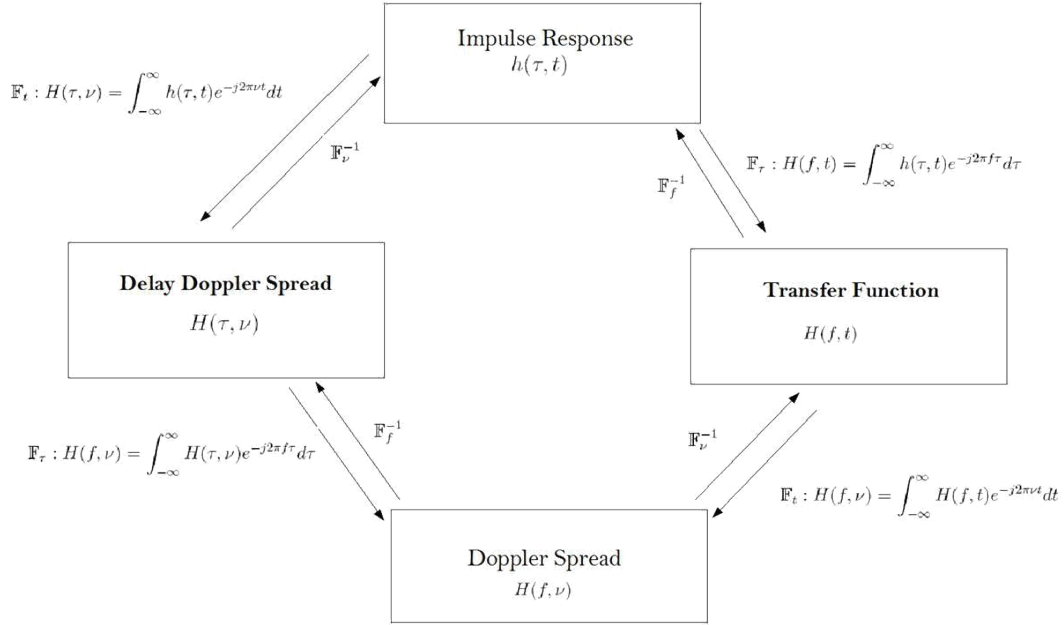


Figure 5.3: Relationship among different channel functions.

where the channel becomes multiplicative.

Doppler spread functions:

$$H(f, \nu) = \text{FT} [H(f, t)] = \int_{-\infty}^{\infty} H(f, t) e^{-j2\pi\nu t} dt \quad (5.31)$$

and

$$H(f, t) = \text{FT}^{-1} [H(f, \nu)] = \int_{-\infty}^{\infty} H(f, \nu) e^{j2\pi\nu t} d\nu \quad (5.32)$$

Delay Doppler spread:

$$H(\tau, \nu) = \text{FT} [h(\tau, t)] = \int_{-\infty}^{\infty} h(\tau, t) e^{-j2\pi\nu t} dt \quad (5.33)$$

Small-Scale Multipath Measurements

Direct RF Pulse System:

A wideband pulsed bistatic radar usually transmits a repetitive pulse of width T_{bb} s, and uses a receiver with a wide bandpass filter ($\text{BW} = \frac{2}{T_{bb}}$ Hz). The signal is then amplified, envelope detected, and displayed and stored on a high speed oscilloscope. Immediate measurements of the square of the channel impulse response convolved with the probing pulse can be taken. If the oscilloscope is set on averaging mode, then this system provides a local average power delay profile.

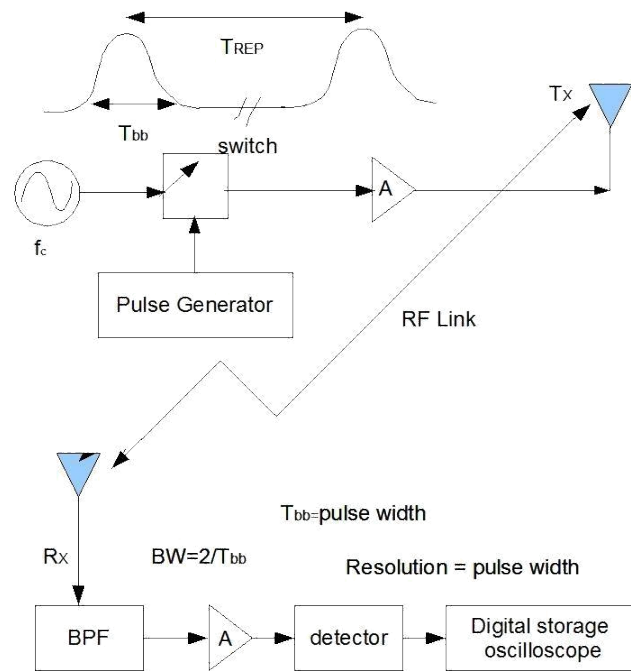


Figure 5.4: Direct RF pulsed channel IR measurement.

This system is subject to interference noise. If the first arriving signal is blocked or fades, severe fading occurs, and it is possible the system may not trigger properly.

Frequency Domain Channel Sounding

In this case we measure the channel in the frequency domain and then convert it into time domain impulse response by taking its inverse discrete Fourier transform (IDFT). A vector network analyzer controls a swept frequency synthesizer. An S-parameter test set is used to monitor the frequency response of the channel. The sweeper scans a particular frequency band, centered on the carrier, by stepping through discrete frequencies. The number and spacing of the frequency step impacts the time resolution of the impulse response measurement. For each frequency step, the S-parameter test set transmits a known signal level at port 1 and monitors the received signal at port 2. These signals allow the analyzer to measure the complex response, $S_{21}(\omega)$, of the channel over the measured frequency range. The $S_{21}(\omega)$ measure is the measure of the signal flow from transmitter antenna to receiver

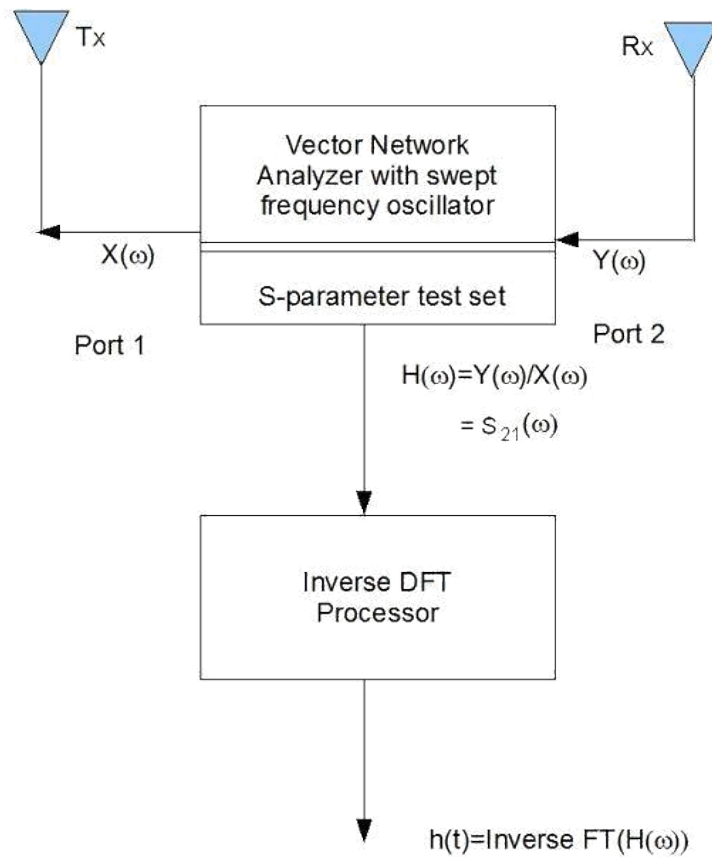


Figure 5.5: Frequency domain channel IR measurement.

antenna (i.e., the channel).

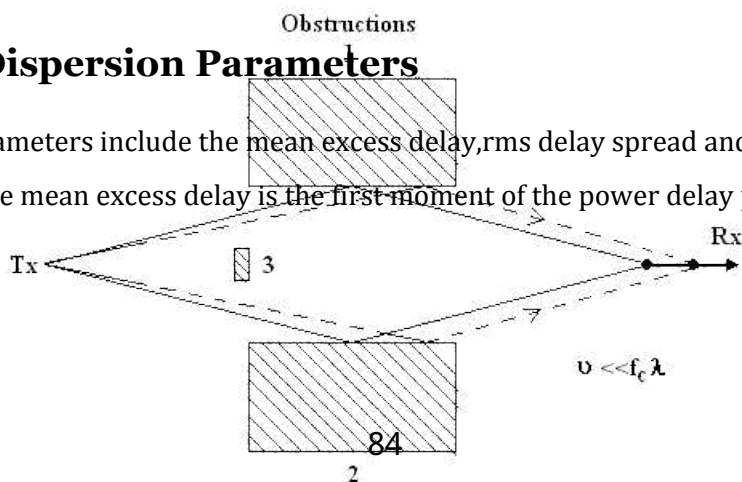
This system is suitable only for indoor channel measurements. This system is also non real-time. Hence, it is not suitable for time-varying channels unless the sweep times are fast enough.

Parameters of Mobile Multipath Channel

To compare the different multipath channels and to quantify them, we define some parameters. They all can be determined from the power delay profile. These parameters can be broadly divided into two types.

Time Dispersion Parameters

These parameters include the mean excess delay, rms delay spread and excess delay spread. The mean excess delay is the first moment of the power delay profile and is



defined as

$$\bar{\tau} = \frac{\sum_k a_k^2 \tau_k}{\sum_k a_k^2} = \frac{\sum_k P(\tau_k) \tau_k}{\sum_k P(\tau_k)} \quad (5.34)$$

where a_k is the amplitude, τ_k is the excess delay and $P(\tau_k)$ is the power of the individual multipath signals.

The mean square excess delay spread is defined as

$$\overline{\tau^2} = \frac{\sum_k a_k^2 \tau_k^2}{\sum_k a_k^2} = \frac{\sum_k P(\tau_k) \tau_k^2}{\sum_k P(\tau_k)} \quad (5.35)$$

Since the rms delay spread is the square root of the second central moment of the power delay profile, it can be written as

$$\sigma_\tau = \sqrt{\overline{\tau^2} - (\bar{\tau})^2} \quad (5.36)$$

As a rule of thumb, for a channel to be flat fading the following condition must be satisfied

$$\frac{\sigma_\tau}{T_s} \leq 0.1 \quad (5.37)$$

where T_s is the symbol duration. For this case, no equalizer is required at the receiver.

Example 2

1. Sketch the power delay profile and compute RMS delay spread for the following:

$$P(\tau) = \sum_{n=0}^1 \delta(\tau - n \times 10^{-6}) \text{ (in watts)}$$

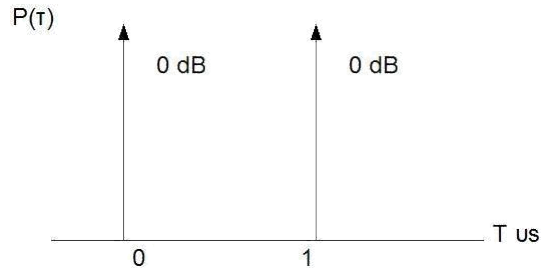
2. If BPSK modulation is used, what is the maximum bit rate that can be sent through the channel without needing an equalizer?

Solution

1. $P(0) = 1 \text{ watt}$, $P(1) = 1 \text{ watt}$

$$\bar{\tau} = \frac{(1)(0) + (1)(1)}{1 + 1} = 0.5 \mu\text{s}$$

$$\tau^2 = 0.5 \mu\text{s}^2 \quad \sigma_\tau = 0.5 \mu\text{s}$$

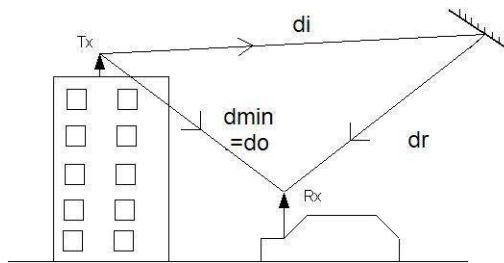


2. For flat fading channel, we need $\frac{\sigma_{\tau}}{T_s} \leq 0.1 \Rightarrow R_s = \frac{1}{T_s} = 0.2 \times 10^4 = 200 \text{ kbps}$

For BPSK we need $R_b = R_s = 200 \text{ kbps}$

Example 3 A simple delay spread bound: **Fehrer's upper bound**

Consider a simple worst-case delay spread scenario as shown in figure below.



Here $d_{min} = d_0$ and $d_{max} = d_i + d_r$

Transmitted power = P_T , Minimum received power = $P_{R_{min}} = P_T$ hreshold

$$P_{R_{min}} = P_T \left(\frac{\lambda}{4\pi d_{max}} \right)^2$$

Put $t_{T} = t_{R} = 1$ i.e., considering omni-directional unity gain antennas

$$d_{max} = \frac{\lambda}{4\pi} \left(\frac{P_T}{P_{R_{min}}} \right)^{\frac{1}{2}}$$

$$\tau_{max} = \frac{d_{max}}{c} = \frac{\lambda}{4\pi c} \left(\frac{P_T}{P_{R_{min}}} \right)^{\frac{1}{2}}$$

$$\tau_{max} = \left(\frac{1}{4\pi f} \right) \left(\frac{P_T}{P_{R_{min}}} \right)^{\frac{1}{2}}$$

Frequency Dispersion Parameters

To characterize the channel in the frequency domain, we have the following parameters.

Coherence bandwidth:

It is a statistical measure of the range of frequencies over which the channel can be considered to pass all the frequency components with almost equal gain and linear phase. When this condition is satisfied then we say the channel to be flat.

Practically, coherence bandwidth is the minimum separation over which the two frequency components are affected differently. If the coherence bandwidth is considered to be the bandwidth over which the frequency correlation function is above

0.9, then it is approximated as

$$B_C \approx \frac{1}{50\sigma_T} \quad (5.38)$$

However, if the coherence bandwidth is considered to be the bandwidth over which the frequency correlation function is above 0.5, then it is defined as

$$B_C \approx \frac{1}{5\sigma_T} \quad (5.39)$$

The coherence bandwidth describes the time dispersive nature of the channel in the local area. A more convenient parameter to study the time variation of the channel is the coherence time. This variation may be due to the relative motion between the mobile and the base station or the motion of the objects in the channel.

Coherence time:

This is a statistical measure of the time duration over which the channel impulse response is almost invariant. When channel behaves like this, it is said to be slow faded. Essentially it is the minimum time duration over which two received signals are affected differently. For an example, if the coherence time is considered to be the bandwidth over which the time correlation is above 0.5, then

it can be approximated as

$$T_C \approx \frac{9}{16\pi f_m} \quad (5.40)$$

where f_m is the maximum doppler spread given by $f_m = \frac{v}{\lambda}$.

Doppler spread:

Another parameter is the Doppler spread (B_D) which is the range of frequencies over which the received Doppler spectrum is non zero.

Types of Small-Scale Fading

The type of fading experienced by the signal through a mobile channel depends on the relation between the signal parameters (bandwidth, symbol period) and the channel parameters (rms delay spread and Doppler spread). Hence we have four different types of fading. There are two types of fading due to the time dispersive nature of the channel.

Fading Effects due to Multipath Time Delay Spread

Flat Fading

Such types of fading occurs when the bandwidth of the transmitted signal is less than the coherence bandwidth of the channel. Equivalently if the symbol period of the signal is more than the rms delay spread of the channel, then the fading is flat fading.

So we can say that flat fading occurs when

$$B_s < B_c \quad (5.1)$$

where B_s is the signal bandwidth and B_c is the coherence bandwidth. Also

$$T_s > \sigma_\tau \quad (5.2)$$

where T_s is the symbol period and σ_τ is the rms delay spread. And in such a case, mobile channel has a constant gain and linear phase response over its bandwidth.

Frequency Selective Fading

Frequency selective fading occurs when the signal bandwidth is more than the coherence bandwidth of the mobile radio channel or equivalently the symbols duration of the signal is less than the rms delay spread.

$$B_s > B_c \quad (5.3)$$

and

$$T_s < \sigma_\tau \quad (5.4)$$

At the receiver, we obtain multiple copies of the transmitted signal, all attenuated and delayed in time. The channel introduces inter symbol interference. A rule of thumb for a channel to have flat fading is if

$$\frac{\sum \tau}{T_s} \leq 0.1 \quad (5.5)$$

Fading Effects due to Doppler Spread

Fast Fading

In a fast fading channel, the channel impulse response changes rapidly within the symbol duration of the signal. Due to Doppler spreading, signal undergoes frequency dispersion leading to distortion. Therefore a signal undergoes fast fading if

$$T_s \gg T_c \quad (5.6)$$

where T_c is the coherence time and

$$T_c \approx \frac{1}{B_D} \quad (5.7)$$

where B_D is the Doppler spread. Transmission involving very low data rates suffer from fast fading.

Slow Fading

In such a channel, the rate of the change of the channel impulse response is much less than the transmitted signal. We can consider a slow faded channel a channel in which channel is almost constant over atleast one symbol duration. Hence

$$T_s \ll T_c \quad (5.8)$$

and

$$B_s \ll B_D \quad (5.9)$$

We observe that the velocity of the user plays an important role in deciding whether the signal experiences fast or slow fading.

Statistical models for multipath propagation

4.7.1 Clarke's Model for Flat Fading

Clarke [Cla68] developed a model where the statistical characteristics of the electromagnetic fields of the received signal at the mobile are deduced from scattering. The model assumes a fixed transmitter with a vertically polarized antenna. The field incident on the mobile antenna is assumed to be comprised of N azimuthal plane waves with arbitrary carrier phases, arbitrary azimuthal angles of arrival, and each wave having equal average amplitude. It should be noted that the equal average amplitude assumption is based on the fact that in the absence of a direct line-of-sight path, the scattered components arriving at a receiver will experience similar attenuation over small-scale distances.

Figure 4.19 shows a diagram of plane waves incident on a mobile traveling at a velocity v , in the x -direction. The angle of arrival is measured in the x - y plane with respect to the direction of motion. Every wave that is incident on the mobile undergoes a Doppler shift due to the motion of the receiver and arrives at the receiver at the same time. That is, no excess delay due to multipath is assumed for any of the waves (flat fading assumption). For the n th wave arriving at an angle α_n to the x -axis, the Doppler shift in Hertz is given by

$$f_n = \frac{v}{\lambda} \cos \alpha_n$$

where λ is the wavelength of the incident wave.

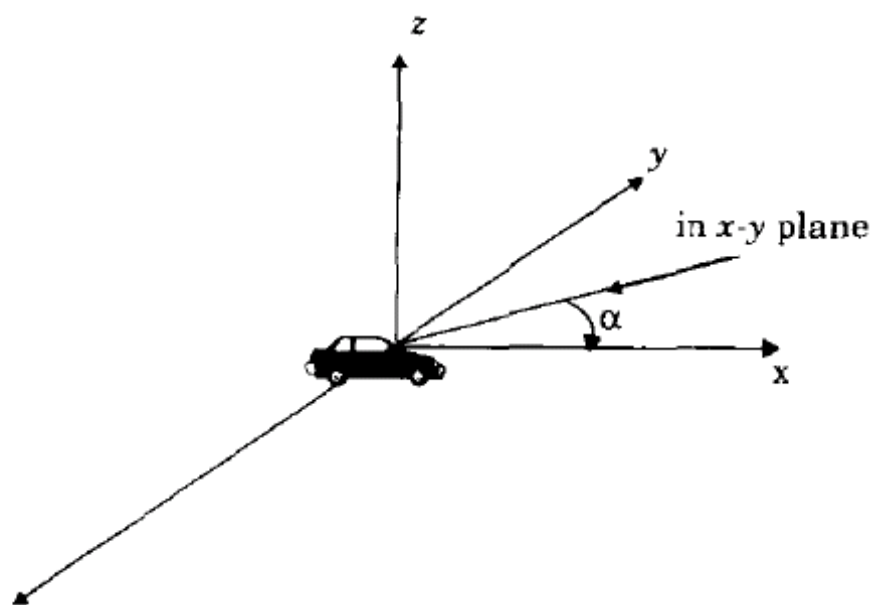


Figure 4.19 Illustrating plane waves arriving at random angles.

The vertically polarized plane waves arriving at the mobile have E and H field components given by

$$\begin{aligned}
E_z &= E_0 \sum_{n=1}^N C_n \cos(2\pi f_c t + \theta_n) \\
H_x &= -\frac{E_0}{\eta} \sum_{n=1}^N C_n \sin \alpha_n \cos(2\pi f_c t + \theta_n) \\
H_y &= -\frac{E_0}{\eta} \sum_{n=1}^N C_n \cos \alpha_n \cos(2\pi f_c t + \theta_n)
\end{aligned}$$

where E_0 is the real amplitude of local average E-field (assumed constant), C_n is a real random variable representing the amplitude of individual waves, η is the intrinsic impedance of free space (377Ω), and f_c is the carrier frequency. The random phase of the n th arriving component θ_n is given by

$$\theta_n = 2\pi f_n t + \phi_n$$

The amplitudes of the E-and H-field are normalized such that the ensemble average of the C_n 's is given by

$$\sum_{n=1}^N \overline{C_n^2} = 1$$

Since the Doppler shift is very small when compared to the carrier frequency, the three field components may be modeled as narrow band random processes. The three components E_z , H_x , and H_y can be approximated as Gaussian random variables if N is sufficiently large. The phase angles are assumed to have a uniform probability density function (pdf) on the interval $(0, 2\pi]$. Based on the analysis by Rice [Ric48] the E-field can be expressed in an in-phase and quadrature form

$$E_z = T_c(t) \cos(2\pi f_c t) - T_s(t) \sin(2\pi f_c t)$$

where

$$T_c(t) = E_0 \sum_{n=1}^N C_n \cos(2\pi f_n t + \phi_n)$$

and

$$T_s(t) = E_0 \sum_{n=1}^N C_n \sin(2\pi f_n t + \phi_n)$$

Both $T_c(t)$ and $T_s(t)$ are Gaussian random processes which are denoted as T_c and T_s , respectively, at any time t . T_c and T_s are uncorrelated zero-mean Gaussian random variables with an equal variance given by

$$\overline{T_c^2} = \overline{T_s^2} = \overline{|E_z|^2} = E_0^2/2$$

where the overbar denotes the ensemble average.

The envelope of the received E-field, $E_z(t)$, is given by

$$|E_z(t)| = \sqrt{T_c^2(t) + T_s^2(t)} = r(t)$$

Since T_c and T_s are Gaussian random variables, it can be shown through a Jacobean transformation [Pap91] that the random received signal envelope r has a Rayleigh distribution given by

$$p(r) = \begin{cases} \frac{r}{\sigma^2} \exp\left(-\frac{r^2}{2\sigma^2}\right) & 0 \leq r \leq \infty \\ 0 & r < 0 \end{cases}$$

where $\sigma^2 = E_0^2/2$

4.7.1.1 Spectral Shape Due to Doppler Spread in Clarke's Model

Gans [Gan72] developed a spectrum analysis for Clarke's model. Let $p(\alpha)d\alpha$ denote the fraction of the total incoming power within $d\alpha$ of the angle α , and let A denote the average received power with respect to an isotropic antenna. As $N \rightarrow \infty$, $p(\alpha)d\alpha$ approaches a continuous, rather than a discrete, distribution. If $G(\alpha)$ is the azimuthal gain pattern of the mobile antenna as a function of the angle of arrival, the total received power can be expressed as

$$P_r = \int_0^{2\pi} A G(\alpha) p(\alpha) d\alpha$$

where $A G(\alpha) p(\alpha) d\alpha$ is the differential variation of received power with angle. If the scattered signal is a CW signal of frequency f_c , then the instantaneous frequency of the received signal component arriving at an angle α is obtained using equation (4.57)

$$f(\alpha) = f = \frac{v}{\lambda} \cos(\alpha) + f_c = f_m \cos \alpha + f_c$$

where f_m is the maximum Doppler shift. It should be noted that $f(\alpha)$ is an even function of α , (i.e., $f(\alpha) = f(-\alpha)$).

If $S(f)$ is the power spectrum of the received signal, the differential variation of received power with frequency is given by

$$S(f) |df|$$

Equating the differential variation of received power with frequency to the differential variation in received power with angle, we have

$$S(f) |df| = A [p(\alpha) G(\alpha) + p(-\alpha) G(-\alpha)] |d\alpha|$$

Differentiating equation (4.70), and rearranging the terms, we have

$$|df| = |d\alpha| |\sin \alpha| f_m$$

Using equation (4.70), α can be expressed as a function of f as

$$\alpha = \cos^{-1} \left[\frac{f - f_c}{f_m} \right]$$

This implies that

$$\sin \alpha = \sqrt{1 - \left(\frac{f - f_c}{f_m}\right)^2}$$

Substituting equation (4.73) and (4.75) into both sides of (4.72), the power spectral density $S(f)$ can be expressed as

$$S(f) = \frac{A [p(\alpha) G(\alpha) + p(-\alpha) G(-\alpha)]}{f_m \sqrt{1 - \left(\frac{f - f_c}{f_m}\right)^2}}$$

where

$$S(f) = 0, \quad |f - f_c| > f_m$$

The spectrum is centered on the carrier frequency and is zero outside the limits of $f_c \pm f_m$. Each of the arriving waves has its own carrier frequency (due to its direction of arrival) which is slightly offset from the center frequency. For the case of a vertical $\lambda/4$ antenna ($G(\alpha) = 1.5$), and a uniform distribution $p(\alpha) = 1/2\pi$ over 0 to 2π , the output spectrum is given by

$$S_{E_z}(f) = \frac{1.5}{\pi f_m \sqrt{1 - \left(\frac{f - f_c}{f_m}\right)^2}}$$

In equation (4.78) the power spectral density at $f = f_c \pm f_m$ is infinite, i.e., Doppler components arriving at exactly 0° and 180° have an infinite power spectral density. This is not a problem since α is continuously distributed and the probability of components arriving at exactly these angles is zero.

Figure 4.20 shows the power spectral density of the resulting RF signal due to Doppler fading. Smith [Smi75] demonstrated an easy way to simulate Clarke's model using a computer simulation as described Section 4.7.2.

After envelope detection of the Doppler-shifted signal, the resulting baseband spectrum has a maximum frequency of $2f_m$. It can be shown [Jak74] that the electric field produces a baseband power spectral density given by

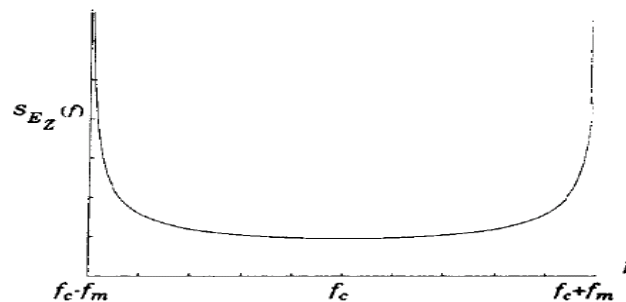


Figure 4.20
Doppler power spectrum for an unmodulated CW carrier [From (Gan72)] © IEEE].

$$S_{bbE_z}(f) = \frac{1}{8\pi f_m} K \left[\sqrt{1 - \left(\frac{f}{2f_m}\right)^2} \right]$$

where $K[\cdot]$ is the complete elliptical integral of the first kind. Equation (4.79) is not intuitive and is a result of the temporal correlation of the received signal when passed through a nonlinear envelope detector. Figure 4.21 illustrates the baseband spectrum of the received signal after envelope detection.

The spectral shape of the Doppler spread determines the time domain fading waveform and dictates the temporal correlation and fade slope behaviors. Rayleigh fading simulators must use a fading spectrum such as equation (4.78) in order to produce realistic fading waveforms that have proper time correlation.

Many multipath models have been proposed to explain the observed statistical nature of a practical mobile channel. Both the first order and second order statistics

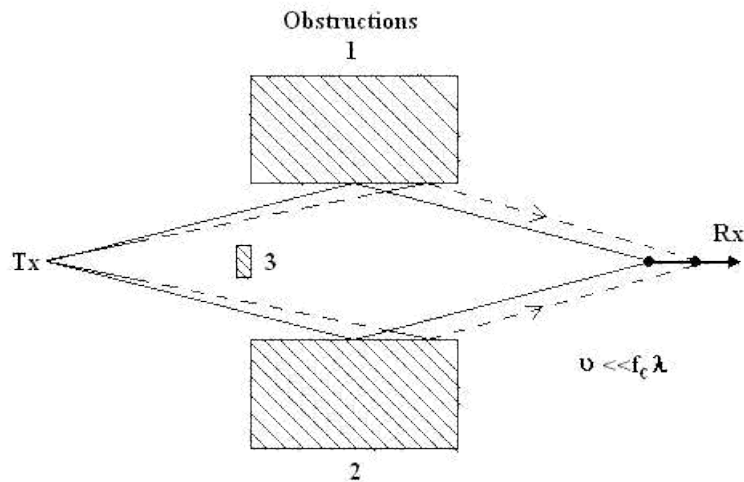


Figure 5.6: Two ray NLoS multipath, resulting in Rayleigh fading.

have been examined in order to find out the effective way to model and combat the channel effects. The most popular of these models are Rayleigh model, which describes the NLoS propagation. The Rayleigh model is used to model the statistical time varying nature of the received envelope of a flat fading envelope. Below, we discuss about the main first order and second order statistical models.

NLoS Propagation: Rayleigh Fading Model

Let there be two multipath signals S_1 and S_2 received at two different time instants due to the presence of obstacles as shown in Figure 5.6. Now there can either be constructive or destructive interference between the two signals.

Let E_n be the electric field and θ_n be the relative phase of the various multipath signals. So we have

$$E = \sum_{n=1}^N E_n e^{j\theta_n}$$

Now if $N \rightarrow \infty$ (i.e. are sufficiently large number of multipaths) and all the E_n are IID distributed, then by Central Limit Theorem we have,

$$\lim_{N \rightarrow \infty} \tilde{E} = \lim_{N \rightarrow \infty} \sum_{n=1}^N E_n e^{j\theta_n} \quad (5.42)$$

$$= Z_r + jZ_i = Re^{j\phi} \quad (5.43)$$

where Z_r and Z_i are Gaussian Random variables. For the above case

$$R = \sqrt{Z_r^2 + Z_i^2} \quad (5.44)$$

and

$$\varphi = \tan^{-1} \frac{Z_i}{Z_r} \quad (5.45)$$

For all practical purposes we assume that the relative phase Θ_n is uniformly distributed.

$$E[e^{j\theta_n}] = \frac{1}{2\pi} \int_0^{2\pi} e^{j\theta} d\theta = 0 \quad (5.46)$$

It can be seen that E_n and Θ_n are independent. So,

$$E[E_n e^{j\theta_n}] = E[E_n] E[e^{j\theta_n}] = 0 \quad (5.47)$$

$$E[E_n^2] = E[E_n e^{j\theta_n} E_n e^{-j\theta_n}] = E[E_n^2 e^{j(\theta_n - \theta_n)}] = E[E_n^2] = P_0 \quad (5.48)$$

where P_0 is the total power obtained. To find the Cumulative Distribution Function(CDF) of R , we proceed as follows.

$$F_R(r) = \Pr(R \leq r) = \int_A f_{Z_i, Z_r}(z_i, z_r) dz_i dz_r \quad (5.49)$$

where A is determined by the values taken by the dummy variable r . Let Z_i and Z_r be zero mean Gaussian RVs. Hence the CDF can be written as

$$F_R(r) = \int_A \frac{1}{2\pi\sigma^2} e^{-\frac{z_r^2 + z_i^2}{2\sigma^2}} dz_i dz_r \quad (5.50)$$

Let $Z_r = p \cos(\theta)$ and $Z_i = p \sin(\theta)$ So we have

$$F_R(r) = \int_0^{2\pi} \int_0^r \frac{1}{2\pi\sigma^2} e^{-\frac{p^2}{2\sigma^2}} p dp d\theta \quad (5.51)$$

$$= 1 - e^{-\frac{r^2}{2\sigma^2}} \quad (5.52)$$

Above equation is valid for all $r \geq 0$. The pdf can be written as

$$f_R(r) = \frac{r}{\sigma^2} e^{-\frac{r^2}{2\sigma^2}} \quad (5.53)$$

and is shown in Figure 5.7 with different σ values. This equation too is valid for all $r \geq 0$. Above distribution is known as Rayleigh distribution and it has been derived

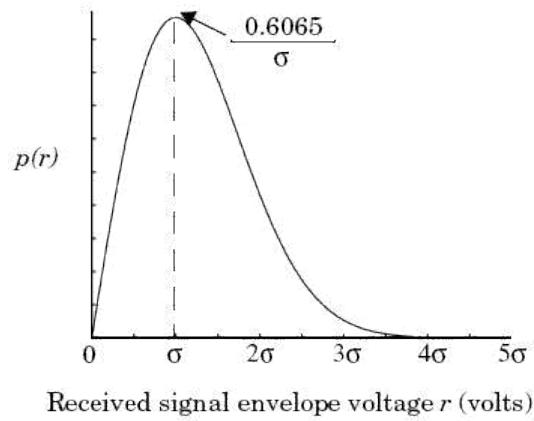


Figure 5.7: Rayleigh probability density function.

for slow fading. However, if $f_D \ll 1$ Hz, we call it as Quasi-stationary Rayleigh fading. We observe the following:

$$E[R] = \frac{\pi}{2} \sigma \quad (5.54)$$

$$E[R^2] = 2\sigma^2 \quad (5.55)$$

$$\text{var}[R] = \left(2 - \frac{\pi}{2}\right) \sigma^2 \quad (5.56)$$

$$\text{median}[R] = 1.77\sigma. \quad (5.57)$$

LoS Propagation: Rician Fading Model

Rician Fading is the addition to all the normal multipaths a direct LOS path.

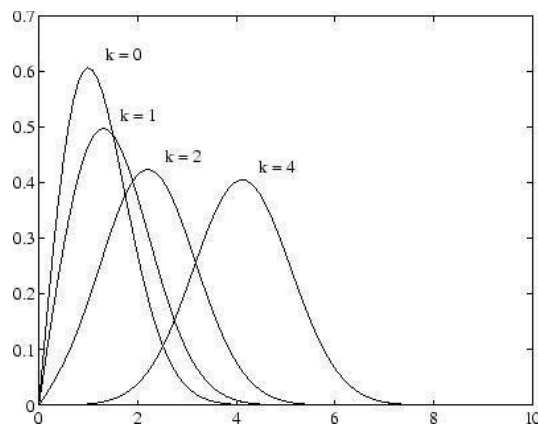


Figure 5.8: Ricean probability density function.

$$f_R(r) = \frac{r}{\sigma^2} e^{-\frac{r^2 + A^2}{2\sigma^2}} I_0\left(\frac{Ar}{\sigma^2}\right) \quad (5.58)$$

for all $A \geq 0$ and $r \geq 0$. Here A is the peak amplitude of the dominant signal and

$I_0(\cdot)$ is the modified Bessel function of the first kind and zeroth order.

A factor K is defined as

$$K_{dB} = 10 \log \frac{A^2}{2\sigma^2} \quad (5.59)$$

As $A \rightarrow 0$ then $K_{dB} \rightarrow \infty$.

Generalized Model: Nakagami Distribution

A generalization of the Rayleigh and Rician fading is the Nakagami distribution.

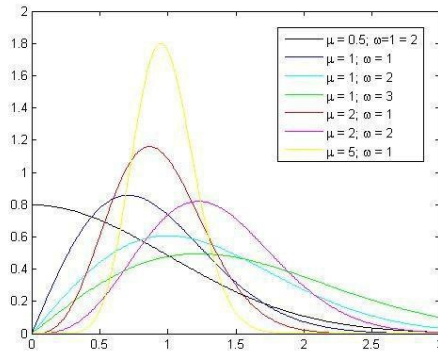


Figure 5.9: Nakagami probability density function.

Its pdf is given as,

$$f_R(r) = \frac{2r^{m-1}}{\Gamma(m) \Omega^m} \left(\frac{m}{\Omega}\right)^m e^{-\frac{mr}{\Omega}} \quad (5.60)$$

where,

$\Gamma(m)$ is the gamma function

Ω is the average signal power and

m is the fading factor. It is always greater than or equal to 0.5.

When $m=1$, Nakagami model is the Rayleigh model.

$$m = \frac{(M+1)^2}{2M+1} \quad \text{When}$$

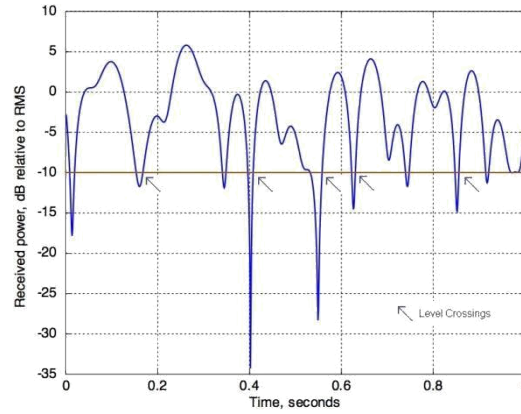


Figure 5.10: Schematic representation of level crossing with a Rayleigh fading envelope at 10 Hz Doppler spread.

where

$$M = \frac{A}{2\sigma}$$

Nakagami fading is the Rician fading.

As $m \rightarrow \infty$ Nakagami fading is the impulse channel and no fading occurs.

Second Order Statistics

To design better error control codes, we have two important second order parameters of fading model, namely the **level crossing rate** (LCR) and **average fade duration** (AFD). These parameters can be utilized to assess the speed of the user by measuring them through the reverse channel. The LCR is the expected rate at which the Rayleigh fading envelope normalized to the local rms amplitude crosses a specific level 'R' in a positive going direction.

$$N_R = \int_0^{\infty} r' p(R, r') dr' = 2\pi f_D \rho e^{-\rho^2} \quad (5.61)$$

where r' is the time derivative of $r(t)$, f_D is the maximum Doppler shift and ρ is the value of the specified level R, normalized to the local rms amplitude of the fading envelope.

The other important parameter, AFD, is the average period time for which the

receiver power is below a specified level R.

$$\tau^- = \frac{1}{N_r} \Pr(r \leq R) \quad (5.62)$$

As

$$\Pr(r \leq R) = \int_0^R p(r) dr = 1 - e^{-\rho^2}, \quad (5.63)$$

therefore,

$$\tau^- = \frac{1 - e^{-\rho^2}}{-\rho^2} \quad (5.64)$$

$$= \frac{2\pi f D \rho e^{-\rho^2}}{2\pi f D \rho} = \frac{1}{2\pi f D \rho} \quad (5.65)$$

Apart from LCR, another parameter is fading rate, which is defined as the number of times the signal envelope crosses the middle value (r_m) in a positive going direction per unit time. The average rate is expressed as

$$N(r_m) = \frac{2v}{\lambda} \quad (5.66)$$

Another statistical parameter, sometimes used in the mobile communication, is called as depth of fading. It is defined as the ratio between the minimum value and the mean square value of the faded signal. Usually, an average value of 10% as depth of fading gives a marginal fading scenario.

Simulation of Rayleigh Fading Models

Clarke's Model: without Doppler Effect

In it, two independent Gaussian low pass noise sources are used to produce in-phase and quadrature fading branches. This is the basic model and is useful for slow fading channel. Also the Doppler effect is not accounted for.

Clarke and Gans' Model: with Doppler Effect

In this model, the output of the Clarke's model is passed through Doppler filter in the RF or through two initial baseband Doppler filters for baseband processing as shown in Figure 5.11. Here, the obtained Rayleigh output is flat faded signal but not frequency selective.

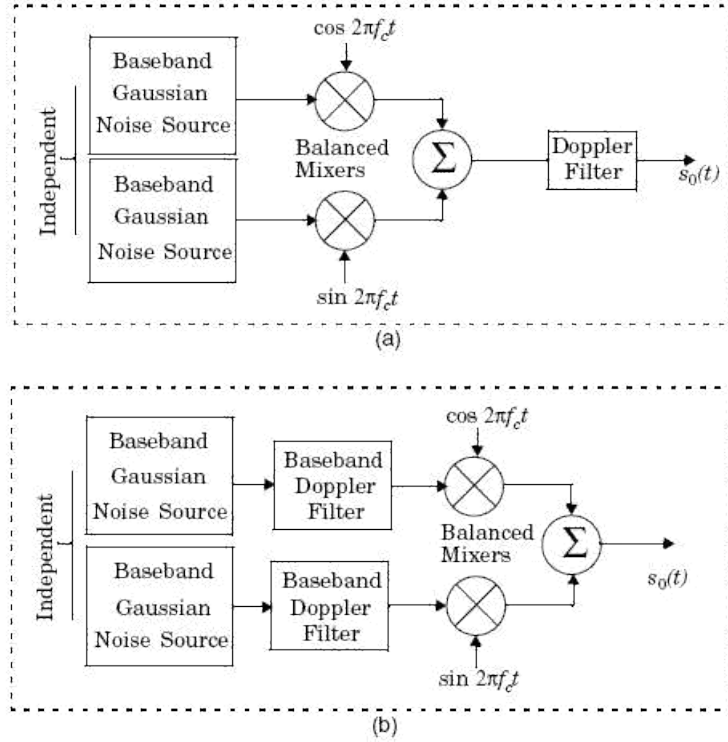


Figure 5.11: Clarke and Gan's model for Rayleigh fading generation using quadrature amplitude modulation with (a) RF Doppler filter, and, (b) baseband Doppler filter.

Rayleigh Simulator with Wide Range of Channel Conditions

To get a frequency selective output we have the following simulator through which both the frequency selective and flat faded Rayleigh signal may be obtained. This is achieved through varying the parameters α_i and τ_i , as given in Figure 5.12.

Two-Ray Rayleigh Faded Model

The above model is, however, very complex and difficult to implement. So, we have the two ray Rayleigh fading model which can be easily implemented in software as shown in Figure 5.13.

$$h_b(t) = \alpha_1 e^{j\varphi_1} \delta(t) + \alpha_2 e^{j\varphi_2} \delta(t - \tau) \quad (5.67)$$

where α_1 and α_2 are independent Rayleigh distributed and φ_1 and φ_2 are independent and uniformly distributed over 0 to 2π . By varying τ it is possible to create a wide range of frequency selective fading effects.

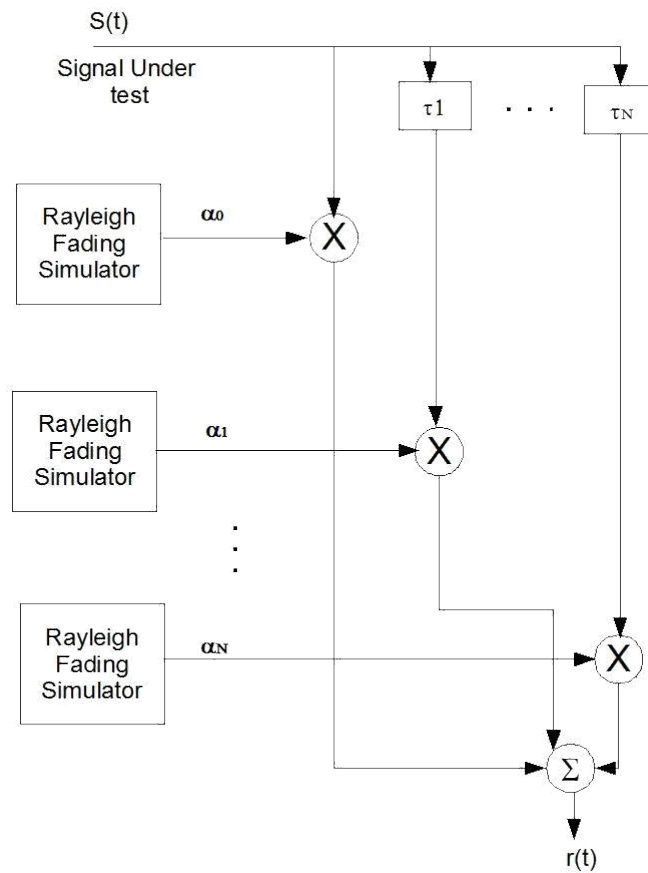


Figure 5.12: Rayleigh fading model to get both the flat and frequency selective channel conditions.

Saleh and Valenzuela Indoor Statistical Model

This method involved averaging the square law detected pulse response while sweeping the frequency of the transmitted pulse. The model assumes that the multipath components arrive in clusters. The amplitudes of the received components are independent Rayleigh random variables with variances that decay exponentially with cluster delay as well as excess delay within a cluster. The clusters and multipath components within a cluster form Poisson arrival processes with different rates.

SIRCIM/SMRCIM Indoor/Outdoor Statistical Models

SIRCIM (Simulation of Indoor Radio Channel Impulse-response Model) generates realistic samples of small-scale indoor channel impulse response measurements. Sub-

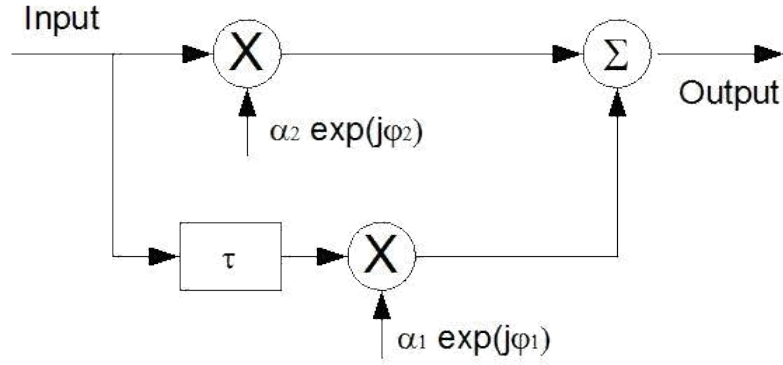


Figure 5.13: Two-ray Rayleigh fading model.

sequent work by Huang produced SMRCIM (Simulation of Mobile Radio Channel Impulse-response Model), a similar program that generates small-scale urban cellular and micro-cellular channel impulse responses.

4.7.3 Level Crossing and Fading Statistics

Rice computed joint statistics for a mathematical problem which is similar to Clarke's fading model [Cla68], and thereby provided simple expressions for computing the average number of level crossing and the duration of fades. The *level crossing rate* (LCR) and *average fade duration* of a Rayleigh fading signal are two important statistics which are useful for designing error control codes and diversity schemes to be used in mobile communication systems, since it becomes possible to relate the time rate of change of the received signal to the signal level and velocity of the mobile.

The *level crossing rate* (LCR) is defined as the expected rate at which the Rayleigh fading envelope, normalized to the local rms signal level, crosses a specified level in a positive-going direction. The number of level crossings per second is given by

$$N_R = \int_0^{\infty} \dot{r} p(R, \dot{r}) d\dot{r} = \sqrt{2\pi} f_m \rho e^{-\rho^2} \quad (4.80)$$

where \dot{r} is the time derivative of $r(t)$ (i.e., the slope), $p(R, \dot{r})$ is the joint density function of r and \dot{r} at $r = R$, f_m is the maximum Doppler frequency and $\rho = R/R_{rms}$ is the value of the specified level R , normalized to the local rms amplitude of the fading envelope [Jak74]. Equation (4.80) gives the value of N_R , the average number of level crossings per second at specified R . The level crossing rate is a function of the mobile speed as is apparent from the presence of f_m in equation (4.80). There are few crossings at both high and low levels, with the maximum rate occurring at $\rho = 1/\sqrt{2}$, (i.e., at a level 3 dB below the rms level). The signal envelope experiences very deep fades only occasionally, but shallow fades are frequent.